ACS SyntheticBiology

Research Article

pubs.acs.org/synthbio

Application of Noncanonical Amino Acids for Protein Labeling in a Genomically Recoded *Escherichia coli*

Kalle Kipper,[†] Ebba G. Lundius,[†] Vladimir Ćurić,[†] Ivana Nikić,[‡] Manfred Wiessler,[∥] Edward A. Lemke,[‡] and Johan Elf*[,†]

[†]Department of Molecular and Cell Biology, Science for Life Laboratory, Uppsala University, Se-751 24 Uppsala, Sweden

[‡]Structural and Computational Biology Unit, Cell Biology and Biophysics Unit, European Molecular Biology Laboratory (EMBL), Heidelberg, 69117, Germany

[∥]Biological Chemistry, Deutsche Krebsforschungszentrum, Heidelberg, 69120, Germany

Supporting Information

ABSTRACT: Small synthetic fluorophores are in many ways superior to fluorescent proteins as labels for imaging. A major challenge is to use them for a protein-specific labeling in living cells. Here, we report on our use of noncanonical amino acids that are genetically encoded via the pyrrolysyl-tRNA/pyrrolysyl-RNA synthetase pair at artificially introduced TAG codons in a recoded *E. coli* strain. The strain is lacking endogenous TAG codons and the TAG-specific release factor RF1. The amino acids contain bioorthogonal groups that can be clicked to externally supplied dyes, thus enabling protein-specific labeling in live cells. We find that the noncanonical amino acid incorporation into the target protein is robust for diverse amino acids and that the usefulness of the recoded *E. coli* strain mainly derives from the absence of release factor RF1. However, the membrane permeable dyes display high nonspecific binding in intracellular environment and the electroporation of hydrophilic nonmembrane permeable dyes severely impairs growth of the recoded strain. In contrast, proteins exposed on the outer membrane of *E. coli* can be labeled with hydrophilic dyes with a high specificity as demonstrated by labeling of the osmoporin OmpC. Here, labeling can be made sufficiently specific to enable single molecule studies as exemplified by OmpC single particle tracking.

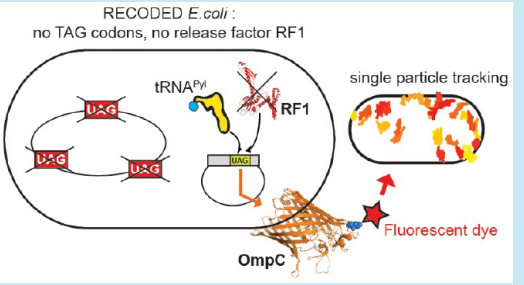

KEYWORDS: *noncanonical amino acid, tetrazine, recoded E. coli, in vivo fluorescence labeling, OmpC, single particle tracking*

Fluorescence microscopy has become one of the most widely used tools in cell and microbiology to study proteins in the context of the living cell. However, since most proteins are not natively fluorescent, they need to be specifically labeled. One of the most widespread methods of *in vivo* protein fluorescence labeling relies on genetically fusing the protein of interest (POI) to natively fluorescent proteins such as green fluorescent protein (GFP) or its derivatives. The chief advantage of the genetic fusion tagging resides in the high chemical specificity; that is, as long as the fusion protein is not degraded all fluorescence will come from the protein of interest (POI). However, a major disadvantage of this approach lies in the large size of the tag which often interferes with the activity of the labeled protein.[1,2] Moreover, due to photobleaching autofluorescent proteins have lower brightness compared to more photostable organic fluorophores, making them less suitable in experiments where many photons are needed from the same protein molecule, which is the case in, for example, single molecule tracking.[3−5] Additionally, localization artifacts have recently been reported for some autofluorescent proteins.[6−8]

Because of the limitations of autofluorescent proteins, much effort has gone into developing alternative methods of protein *in vivo* labeling using small synthetic fluorophores. Although differing in the chemistry of the dye attachment site (referred to as "labeling handle") in the POI, the attachment site is genetically encoded in all those small fluorophore-based labeling schemes to enable labeling specificity. The "handle" may comprise an entire dye reactive protein as exemplified by the SNAP,[9] CLIP,[10] HALO,[11] and DHFR[12,13] tagging technologies or may be a short peptide sequence embedded in the POI as in the case of sortase-,[14] ligase-,[15−19] or Flash-[20−24] tagging. Though providing a way of incorporating tailor-made fluorophores with superior photophysical properties into proteins *in vivo*, nonspecific fluorescence incoporation into cells has been noted with some of those methods.[25−27] Additionally, with the SNAP/CLIP/HALO and DHFR tags, which have a size close to that of the autofluorescent proteins, there is still the danger of the tag interfering with the activity of the POI. This risk is reduced with the enzyme mediated peptide tagging as developed by Ting and colleagues.[15] This labeling technique allows the conjugation of short peptide sequences in proteins with biotin or lipoic acid derivatives using biotin or

Received: May 3, 2016
Published: October 24, 2016

DOI: 10.1021/acssynbio.6b00138
ACS Synth. Biol. XXXX, XXX, XXX−XXX

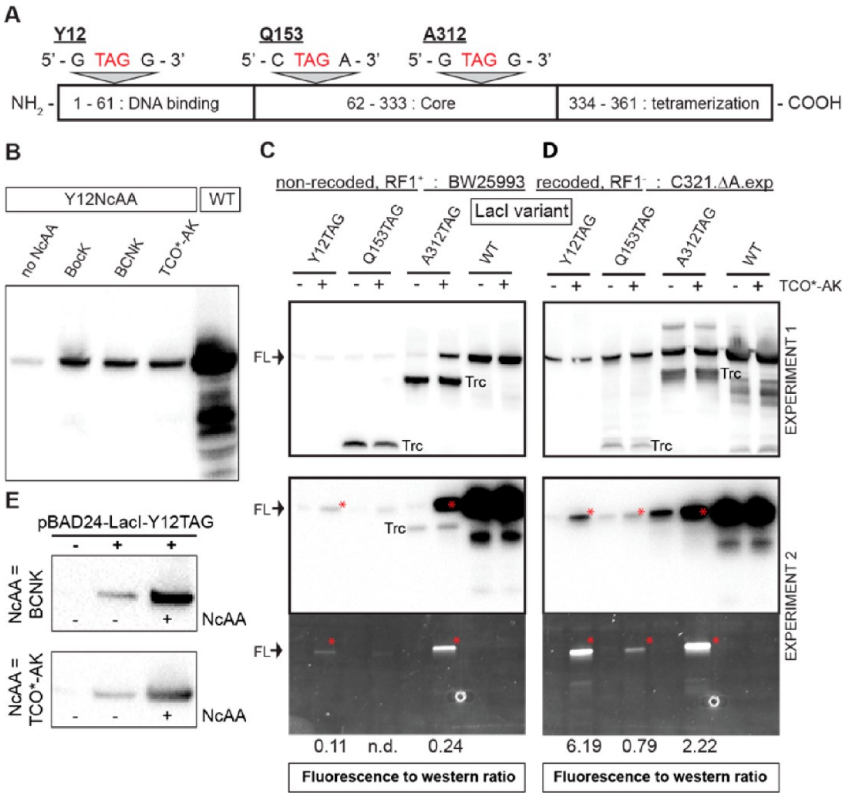

Figure 1. NcAA-dependent expression of LacI. (A) NcAA-incoporation sites in LacI. The location of the TAG stop codon in the LacI constructs is shown alongside with the 5′- and 3′- flanking nucleotides. (B) *E. coli* C321.ΔA.exp cells transformed with pEVOL and pBAD24-LacI-Y12TAG were grown in the presence of 0.02% L-arabinose and 1 mM of different NcAAs for 5 h at 37 °C. Cells were lyzed and lysates resolved by SDS-PAGE. LacI expression was visualized by Western blot using a LacI-specific antibody. (C and D) Analysis of NcAA-incorporation in *E. coli* strains C321.ΔA.exp and BW25993, respectively. Cells transformed with pEVOL and one of the pBAD24-LacI constructs were grown in LB at 37 °C in the presence of 1 mM TCO*-AK. LacI expression was induced with 0.02% L-arabinose and the cells were harvested for lysis at ΔOD600 = 0.9. LacI was labeled in lysate supernatants with 1 μM ATTO647N-tet at 37 °C for 30 min. LacI expression and labeling were analyzed by Western blot and in-gel fluorescence, respectively. "FL", full-length LacI; "Trc", truncated LacI. The Western blots are from two independent experiments (EXPERIMENTS 1 and 2). The fluorescence gel is from EXPERIMENT 2. The numbers below the fluorescent LacI lanes denote the ratio of the fluorescence signal in the fluorescent LacI band (marked with asterisk) normalized to the luminescence signal in the corresponding full-length LacI band (marked with asterisk) in the Western blot. (E) The Western blot band in (D) in the absence of NcAA is not caused by detecting endogenous LacI. C321.ΔA.exp cells with or without pBAD24-LacI-Y12TAG were grown in LB at 37 °C for 5 h in the presence or absence of 1 mM NcAA and 0.02% L-arabinose. LacI expression was detected using a LacI-specific antibody.

lipoic acid ligase.[15,28] These derivatives carry, for example, azide or alkyne functionalities that allow conjugation with fluorophores using "click" chemistry.[29] Though initially restricted to labeling proteins on the cell surface[15] because of cross-reactivity with endogenous substrates, engineering of these enzymes has led to the development of ligases with low cross-reactivity[17] and an ability to directly incorporate fluorophores into proteins in the intracellular environment.[17,19]

To further minimize the size of the fluorescent label while retaining its genetic encoding, a strategy of cotranslationally incorporating a noncanonical amino acid (NcAA) with a fluorescent side chain has been developed by Schultz and co-workers.[30,31] The fluorescent NcAA is incorporated at an artificially introduced amber (TAG) stop codon in the gene of the POI using an evolved suppressor tRNA/aminoacyl-tRNA synthetase pair.[30,31] Because of the small size of the NcAA there is a considerable freedom in the placement of the label within the POI compared to the enzymatic or even peptide tags. This NcAA-based labeling strategy was successfully used by Chapman and co-workers to label the bacterial cytoskeletal protein FtsZ and characterize its cellular localization.[32] However, such a direct incorporation of fluorescent amino acids is currently not suited for the incorporation of bulkier but photophysically superior fluorophores due to an inefficient accommodation and delivery of those fluorophores to the ribosome.[33] To address these challenges, the NcAA-based protein labeling scheme has been substituted with a two-step protocol where a relatively small nonfluorescent NcAA is first genetically incorporated at the amber stop codon and then conjugated with a fluorescent dye.[34−38] The side chains of the NcAAs contain ring-strained functional groups[39,40] that react with tetrazine (tet)-containing fluorophores in different types of catalyst-free strain-promoted cycloaddition reactions.[41−45] Since the reaction between tetrazine and the ring-strained moiety in the NcAA is highly specific,[46] spurious labeling of endogenous proteins is avoided.[47] The NcAAs are incorporated using an archeal $tRNA^{Pyl}$-(where Pyl stands for pyrrolysine, the 22nd natural amino acid) or $tRNA^{Tyr}$ derived suppressor tRNA charged with the NcAA by the cognate synthetase.[48−51] As neither the suppressor tRNA nor its cognate aminoacyl-tRNA synthetase participate in endogenous aminoacylation reactions[49,52] (i.e., the suppressor tRNA and the synthetase are orthogonal to the expression host[53,54]), ideally only the NcAA is attached to the suppressor tRNA.[49,52] The overall specificity

DOI: 10.1021/acssynbio.6b00138
ACS Synth. Biol. XXXX, XXX, XXX−XXX

of the NcAA-based labeling thus derives both from the specific encoding of the NcAA by the $tRNA^{Pyl}$/PylRS pair and from the chemical specificity of the cycloaddition reaction between the NcAA and the tetrazine moiety in the fluorophore.[44,46,55] A factor that potentially restricts the specificity of the NcAA-based labeling scheme resides in the encoding of the NcAA by the amber stop codons which are present throughout the genomes of most model organisms. Thus, as long as the endogenous amber codons are present, one may anticipate a certain level of "off-target" incorporation of the NcAA into the proteome of the expression host, leading to a concomitant nonspecific incorporation of the fluorophore. Fortunately, in the case of *E. coli*, a genetically recoded derivative of the MG1655 strain is now available where all the known endogenous amber stop codons have been replaced with the alternative ochre stop codon TAA.[56] This recoding leaves the artificially introduced TAG codon in the gene of POI as the only specific codon to be read by the NcAA-$tRNA^{Pyl}$. The NcAA-based labeling approach is therefore at least in theory suitable to live cell fluorescence microscopy studies in *E. coli*. However, while having been successfully applied to protein labeling in eukaryotic cells, there are as yet few reports in recoded organisms.

We report on our efforts to label different intra- and extracellular proteins with synthetic fluorophores in the recoded *E. coli* using the NcAA-based small fluorophore tagging. We have applied this labeling scheme to proteins that are difficult to tag with autofluorescent proteins without compromising their biological function, in particular the *lac* operon repressor LacI. LacI is natively a tetramer but labeling with yellow fluorescent protein (YFP) in the C-terminal makes it a dimer[57] and labeling in the N-terminus prevents it from binding DNA. We have been able to characterize how the YFP labeled dimer searches for its chromosomal DNA targets in great detail.[57−59] However, the tetramer is suggested to have different search modes[60] and an NcAA-based small fluorophore tagging of LacI may allow us to explore these in living cells. We find that the labeling of the intracellular proteins suffers from high background fluorescence due to the nonspecific intracellular binding by the more membrane permeable hydrophobic fluorophores and from the restricted membrane permeability of the more hydrophilic fluorophores. However, proteins exposed on the outer surface of the *E. coli* cells are amenable for labeling as shown by our specific labeling of the outer membrane porin OmpC. Using fluorescent dyes as labels for OmpC, we were able to follow its lateral diffusion over trajectory lengths far exceeding those obtainable with autofluorescent protein tags. OmpC lateral diffusion was largely confined to zones of 0.5 μm radii or less with rare excursions out of the confinement zone. We conclude that to be a viable alternative to the fusion tag labeling for intracellular proteins in *E. coli*, the fluorophores must be improved with regard to their membrane permeability/nonspecific binding. For example "turn-on" dyes that become fluorescent upon the "click" reaction[61−63] seem to be a promising direction that would circumvent some of those problems.

RESULTS AND DISCUSSION

NcAA Incorporation. Variants of LacI and OmpC harboring site-specifically incorporated NcAAs were expressed from amber (TAG) codon containing constructs in pBAD24 in the presence of 1 mM NcAA and the *Methanosarcina mazei* $tRNA^{Pyl}_{CUA}$/$PylRS^{AF}$ pair (Supporting Information, Table S1) encoded in the plasmid pEVOL.[64] $PylRS^{AF}$ is a double mutant (Y306A, Y384F) of *M. Mazei* PylRS synthetase designed for a more efficient recognition of bulky NcAAs.[34] The pEVOL plasmid (from ref 34) harbors two copies of the $PylRS^{AF}$. One of the PylRS copies is under the control of the arabinose inducible *araBAD* promoter while the other copy of $PylRS^{AF}$ is constitutively expressed from the *gln S′* promoter.[64] The NcAA incorporation and dye labeling experiments were, unless stated otherwise, performed in the recoded *E. coli* strain C321.ΔA.exp[56] in which all known endogenous TAG codons have been replaced with the TAA stop codon and the TAG-specific release factor RF1 has been deleted. The NcAA incorporation sites were selected based on existing mutagenesis data as follows. In LacI, the NcAA incorporation sites (Figure 1A) were selected using the data of Miller and co-workers from an amber suppression-based substitution tolerance analysis.[65,66] In OmpC,[67] the NcAA incorporation site was introduced in the cell surface exposed loop 7.[68] This loop has been previously used for inserting exogenous polypeptide sequences into OmpC.[69] Out of the residues in loop 7, position 311 was selected for the NcAA incorporation based on its low conservation score in the amino acid conservation analysis as determined using the ConSurf web server[70] (Supporting Information, Figure S1). For both LacI and OmpC, the surface accessibility of the selected position for dye labeling was verified by an inspection of the protein structures (Figure S1). For the NcAA incorporation we used the tetrazine-unreactive (i.e., "nonclickable") amino acid eBoc-lysine (eBocK) as well as the tetrazine reactive (i.e., "clickable") amino acids endobicyclo[6.1.0]nonyne-lysine (endo-BCNK) and the axial isomer of *trans*-cyclooct-2-ene-lysine (TCO*-AK) (Figure S2). For the sake of clarity we will refer to proteins containing a tetrazine reactive NcAA as "clickable" and to proteins containing a tetrazine unreactive NcAA as "unclickable". A protein of interest containing a tetrazine unreactive endogenous amino acid at the position reserved for the NcAA will be referred to as "wild-type" (WT). With regard to tetrazine reactivity the WT protein is also "unclickable". We preferred TCO*-AK over other "clickable" NcAAs due to its efficient recognition by the PylRS synthetase,[37] superior stability in the presence of intracellular thiols,[37,71] and its high labeling efficiency with 1,2,4,5-tetrazine fluorophores.[71] We note that TCO*-AK tetrazine adducts have been reported to be susceptible to elimination and the ensuing loss of the pyridazine leaving group from lysine.[72,73] Though this elimination would potentially compromize the labeling yield of a TCO*-AK containing protein with tetrazine dyes, a recent study by Hoffmann and colleagues places this loss within 10%−30% and concludes that this unfavorable elimination reaction is compensated by the overall higher incorporation and labeling yield of TCO*-AK with tetrazines,[71] making TCO*-AK a good choice when fast protein labeling at low tetrazine dye concentration is required.

NcAA Incorporation Efficiency into LacI Is Position-Dependent. We first evaluated the NcAA incorporation efficiency by monitoring the expression of LacI ("LacI-Y12NcAA") from a construct containing an artificially introduced TAG stop codon at amino acid position 12 (Figure 1A) in the presence of 1 mM eBocK, BCNK or TCO*-AK. Despite differences in the size and chemical reactivity of the NcAAs (Figure S2) the expression levels of the LacI-Y12NcAA variant were similar to the three NcAAs (Figure 1B) and remained markedly below the expression level of the WT LacI

DOI: 10.1021/acssynbio.6b00138
ACS Synth. Biol. XXXX, XXX, XXX−XXX

Table 1. Physicochemical Characteristics of the Tetrazine Dyes Used in the Study

dye	λ_{MAX} [a] (em)	λ_{MAX} [a] (ex)	ε [a] ($M^{-1}cm^{-1}$)	Net charge [b] at pH 7.4	logD [c] at pH 7.4	length of linker (atoms)	substituent at tetrazine C6	substituent electron donating	substituent electron withdrawing
ATTO532-tet	553 nm	532 nm	115 000	−1.92	−2.64	7	H-		
ATTO647N-tet	644 nm	669 nm	150 000	1.00	4.52	2	H-		
Cy5-tet	n.a.	n.a.	n.a.	1.00	5.24	12	2-pyrimidinyl-		+
Sulfo-Cy5-tet	649 nm	670 nm	250 000	−1.00	2.20	12	H-		
m6-sulfo-Cy5-tet	647 nm	663 nm	251 000	−2.00	−0.35	12	CH_3-	+	
TAMRA-tet	545 nm	563 nm	89 000	0.00	0.71	14	CH_3-	+	

[a]Data provided by the manufacturer. [b]Calculated from structures using "Marvin Sketch" version 16.6.27 software (Chemaxon). [c]Calculated for the major microspecies at pH 7.4 using "Marvin Sketch" 16.6.27 software. Notation: n.a., data not available.

variant (Figure S3). The expression of LacI-NcAA could be first detected within 2 h of starting the induction (Figure S4). The similar incorporation efficiencies of the chemically diverse NcAAs into LacI are consistent with the NcAA incorporation analysis of Summerer and co-workers where the suppression efficiency of the *M. jannaschii* $tRNA^{Pyl}$/PylRS system was little affected by differences in the chemical structures of the NcAA.[74] In contrast to the similar expression levels of LacI-NcAA with structurally diverse NcAAs, the expression levels of LacI-NcAA varied depending on the location of the TAG codon in the *lacI* gene (Figure 1C). This effect was more notable in the nonrecoded *E. coli* strain BW25993 (Figure 1C,D). The highest level of LacI-TCO*-AK expression was observed with a construct harboring the TAG codon at the amino acid position 312 in both strains (Figure 1C,D). However, the expression levels of the three LacI-NcAA variants were less variable in the recoded strain C321.ΔA.exp (Figure 1D). Though the incorporation efficiency of an NcAA by the $tRNA^{Pyl}$/PylRS system may be influenced by multiple factors, codon context appears to be the most important factor as revealed by a recent analysis of Xu and co-workers.[75] A comparison of the codon context around the three TAG codons in LacI with the data of Xu and co-workers[75] revealed that none of the TAG codons in our LacI constructs is flanked by the most favorable sequences for $tRNA^{Pyl}$ decoding. This suboptimal codon context may be one reason for the relatively low expression levels of the NcAA-LacI variants compared to the expression level of WT LacI (Figure 1B).

Protein Truncation Is More Pronounced in the Presence of RF1. In the $RF1^+$ strain BW25993, Western blot analysis of LacI expression from the LacI-Q153TAG and LacI-A312TAG constructs revealed the presence of an additional protein species. This additional protein had the size expected of LacI truncated at the artificial TAG codon (Figure 1C, Figure S5A). In the case of the Y12TAG construct the formation of a possible truncation product could not be analyzed by Western Blot due to its small size (11 amino acids). In contrast, a less extensive protein truncation was observed in the $RF1^-$ strain C321 (Figure 1D, Figure S5B). Before moving on to the dye labeling results we note that when the LacI-NcAA expressing cells were treated with tetrazine dyes no fluorescent species corresponding to the truncated protein was seen in either of the strains (Figure 1C,D). This observation suggests that the truncation occurs before the NcAA incorporation and is probably a result of the RF1-mediated release of the nascent polypeptide at the artificial TAG codon. In line with this, expression of LacI from the TAG containing construct in the absence of the NcAA slowed down cell growth relative to expressing LacI from the WT construct (Figure S6). This effect was also more pronounced in the $RF1^+$ BW25993 strain (Figure S6). On the basis of these observations, we suggest that the less extensive protein truncation in the C321.ΔA.exp strain (Figure 1D) is due to the absence of RF1, in agreement with the results of Johnson and co-workers.[76] Moreover, the fact that the formation of the truncated LacI was reduced in the RF1 deletion strain C321.ΔA.exp indicates that the misreading of the premature TAG codon by the noncognate release factor RF2 is not significantly increased in the absence of RF1 contrary to what has been recently observed *in vitro*.[77]

NcAA-Independent Read-through of the UAG Codon Is Increased in Recoded E. coli. In the C321 strain, Western blot analysis revealed LacI expression from the LacI-Y12TAG and LacI-A312TAG constructs in the absence of the NcAA (Figure 1D). The NcAA-independent LacI expression from the TAG containing constructs was lower in cells harvested from stationary phase (ΔOD600 = 3−6) cultures (Figure S5B) compared to cells harvested at ΔOD600 = 0.9 (Figure 1D). Control experiments in cells lacking LacI expression constructs confirmed that this NcAA-independent full-length LacI synthesis is not due to the detection of endogenous LacI (Figure 1E). The NcAA-independent expression of LacI may be due to a misincorporation of an endogenous amino acid into LacI by (i) either a promiscuous activity of the $PylRS^{AF}$ synthetase in accepting an endogenous amino acid or (ii) an enhanced endogenous amber suppression in the absence of RF1 as observed in previous reports.[56,76,78] Since the NcAA-independent expression of LacI was more prominent in the RF1 knock out strain C321.ΔA.exp (Figure 1D) compared to the $RF1^+$ strain BW25993 (Figure 1C) we favor explanation ii as PylRS would likely display a promiscuous activity regardless of the expression host. Regardless of the mechanism of the NcAA-independent LacI synthesis, it would potentially compromize the subsequent dye labeling of the protein by reducing the level of LacI-NcAA. Nevertheless, dye treatment of cells harvested from an NcAA containing LacI expression culture resulted in a fluorescently labeled LacI in in-gel analysis (Figure 1C,D). This indicates that despite an increased competition from the misincorporation of endogenous amino acids at the artificial TAG codon in C321.ΔA.exp the $tRNA^{Pyl}$/PylRS system is able to produce the "clickable" protein at levels resulting in detectable fluorescently labeled product.

Dye Labeling. *Cell Membrane Affects the Efficiency of Intracellular Protein Labeling.* To find suitable dye(s) for live cell protein labeling we first analyzed the efficiency of protein labeling with different 1,2,4,5-tetrazine containing fluorophores by in-gel fluorescence. We preferred tetrazine containing dyes to, for example, azide dyes due to the magnitudes faster rates and the irreversibility of the tetrazine reactions.[41,44,46,55] We used the commercially available tetrazine derivatives of ATTO647N, TAMRA, sulfo-Cy5 (commonly referred to as

DOI: 10.1021/acssynbio.6b00138
ACS Synth. Biol. XXXX, XXX, XXX−XXX

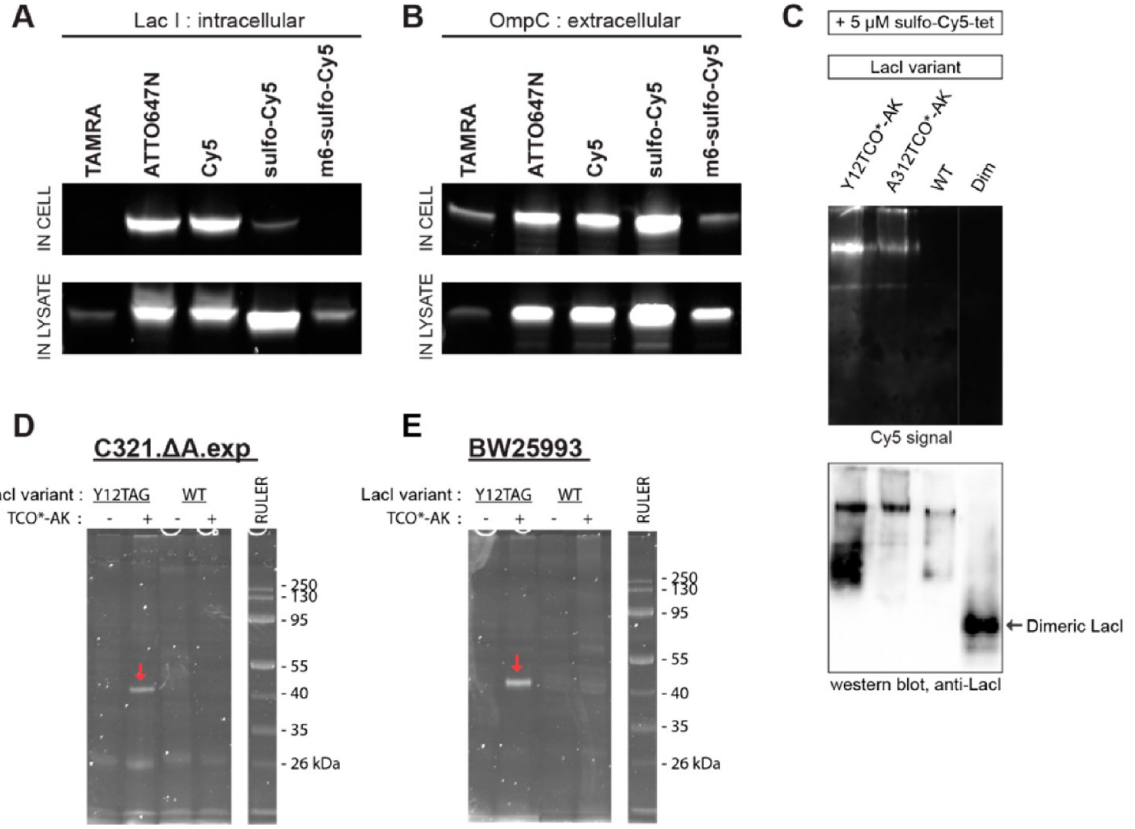

Figure 2. In-gel analysis of protein labeling with tetrazine fluorophores. (A and B). Comparison of intra- (LacI) (A) and extracellular (OmpC) (B) protein labeling in intact cells and cell lysates. C321.ΔA.exp cells transformed with pEVOL and pBAD24-LacI-Y12TAG or pBAD24-OmpC-D311TAG were grown in LB in the presence of 1 mM TCO*-AK at 37 °C and harvested at ΔOD600 = 0.8 (OmpC) or 1.8 (LacI). After a copious washout of excess TCO*-AK and cell lysis intact cells and cell lysates were treated with 5 μM of tetrazine fluorophores at 37 °C for 30 min. Proteins from cells and lysates were resolved by SDS-PAGE and analyzed for in-gel fluorescence. (C) Impact of dye labeling on LacI tetramerization. Affinity purified, N-terminally His6-tagged LacI variants were incubated with 5 μM sulfo-Cy5-tet at 37 °C for 30 min, and the labeling products were resolved by native PAGE. LacI expression was confirmed by Western blot. "Dim" denotes a C-terminally His6-tagged variant of LacI where the C-terminal tetramerization helix has been removed. (D and E) Analysis of "off-target" fluorescence incoporation into cellular proteome in C321.ΔA.exp and BW25993, respectively. Cells expressing LacI from the Y12TAG and WT constructs in the presence of 1 mM TCO*-AK were grown in LB at 37 °C and harvested for lysis at ΔOD600 = 2. The lysates were incubated with 1 μM ATTO647N-tet for 30 min at 37 °C, and the labeling products were analyzed by SDS-PAGE on a 12% acrylamide gel. Red arrow denotes the labeled LacI.

simply "Cy5" but consistently referred to as "sulfo-Cy5" throughout this publication) and m6-sulfo-Cy5 as well as a custom synthesized sulfo-group free derivative of Cy5[79] (hereafter referred to as "Cy5") (Figure S7). The advantage of commercially available tetrazine fluorophores lies in their accessibility to researchers without in-house organic synthesis facilities. Our preference for the red light excitable dyes was motivated by the lower cellular autofluorescence in the red spectral region. The tetrazine groups in the selected dyes contain substituents with different electron donating/withdrawing propensities (Table 1; Figure S7). Though electron donating substituents (including the methyl group in m6-sulfo-Cy5-tet and TAMRA-tet) are known to decrease tetrazine reactivity in strain-promoted [4 + 2] cycloadditions,[42] they have the advantage of increasing the solvent stability of tetrazines.[42] The slower reacting 6-methyl substituted tetrazine dyes m6-sulfo-Cy5-tet and TAMRA-tet were therefore included in the analysis as a successful *in vivo* protein labeling may require a trade-off between the reactivity and chemical stability of the tetrazine group in the fluorophore. Furthermore, on the basis of previous information on the membrane permeability of small molecules[80] we anticipated that the labeling efficiencies of intracellular proteins (as exemplified by LacI) with the tetrazine fluorophores may be influenced by the different membrane permeabilities of the dyes. To separate the effects of membrane permeability from the intrinsic differences in the chemical reactivities of the tetrazine fluorophores, protein labeling was performed in parallel with LacI and the cell surface exposed protein OmpC.[67,68] In the case of OmpC the accessibility of the target protein to the dyes is not compromised by the cell membranes, and the differences in the labeling yields would reflect the intrinsically different reactivities of the tetrazine groups.

In intact cells the highest labeling yields were observed with ATTO647N-tet and Cy5-tet with both the intracellularly located LacI-Y12TCO*-AK (Figure 2A) and the surface exposed OmpC-D311TCO*-AK (Figure 2B). The labeling yields with ATTO647N-tet and Cy5-tet were similar on both proteins (Figure 2A,B). Since the linker between the fluorophore and tetrazine moieties is shorter in ATTO647N-tet compared to Cy5-tet (Table 1; Figure S7), the similar labeling yield regardless of the linker length indicates that the distance of the fluorophore to the tetrazine does not markedly affect the attachment of the dye to the protein-bound NcAA. With sulfo-Cy5-tet the labeling yield was similar to that observed with ATTO647N-tet and Cy5-tet when the cell

DOI: 10.1021/acssynbio.6b00138
ACS Synth. Biol. XXXX, XXX, XXX−XXX

surface exposed OmpC-D311TCO*-AK was labeled in intact cells (Figure 2B) and concentrations of sulfo-Cy5-tet as low as 10 nM resulted in a detectable fluorescent OmpC band (Figure S8). In contrast, with the intracellularly located LacI-Y12TCO*-AK the labeling with sulfo-Cy5-tet in intact cells was less efficient compared to ATTO647N-tet and Cy5-tet (Figure 2A). With TAMRA-tet and m6-sulfo-Cy5-tet the yields were significantly lower compared to the other dyes in OmpC-D311TCO*-AK labeling (Figure 2B) and essentially no labeling with TAMRA-tet and m6-sulfo-Cy5-tet was observed in the case of LacI-Y12TCO*-AK (Figure 2A). A similar trend in the labeling efficiencies of the selected dyes was observed when the labeling was performed in cell lysates (Figure 2A,B). In lysates the only exception was the labeling of LacI with sulfo-Cy5-tet where the yield was now similar to that obtained with ATTO647N-tet and Cy5-tet (Figure 2A). The similar labeling yields with ATTO647N-tet and Cy5-tet in the case of both LacI (an intracellular protein) and OmpC (a surface exposed protein) in intact cells indicate that the cell membranes do not restrict the accessibility of the target protein to those dyes. We speculate that in contrast to the negatively charged sulfo-Cy5-tet and m6-sulfo-Cy5-tet the positively charged of ATTO647N-tet and Cy5-tet (Table 1) are not repelled by the anionic groups on the outer leaflet of the *E.coli* outer membrane while the relatively high hydrophobicity of those dyes (as evidenced by the large positive partition coefficient, logD) (Table 1) facilitates their diffusion through the phospholipid membranes. In contrast, the reduced labeling efficiency of LacI with the negatively charged sulfo-Cy5-tet in intact cells compared to labeling in lysate may be due to the repulsion of sulfo-Cy5-tet by the anionic groups on the *E.coli* outer membrane. On the other hand, the low labeling yields of LacI with TAMRA-tet and m6-sulfo-Cy5-tet, even in the absence of cell membranes, indicate their intrinsically lower chemical reactivities, consistent with the presence of the electron donating methyl substituent on the tetrazine groups of those dyes.[42] We note though that when the labeling of LacI-Y12TCO*-AK with the more permeable dyes ATTO647N-tet and Cy5-tet was compared in exponential and stationary phase cells, nearly identical labeling yields were observed in samples derived from both growth phases despite the markedly higher expression level of LacI-Y12TCO*-AK in the stationary phase cells (Figure S9). This observation suggests that the cell membrane in stationary phase cells is less permeable to the dyes compared to the exponential phase. Consistent with the previously reported high rates of the strain promoted cycloaddition reactions of tetrazines,[35,37] the labeling of LacI and OmpC with ATTO647N-tet was essentially complete within 5 min of the dye addition in both intact cells and cell lysates (Figure S10A,B).

Dye Labeling Does Not Interfere with the Tetramerization of LacI. An appealing aspect of the small molecule labeling is that the small size of the fluorescent dye makes it less likely to interfere with the folding and biological activity of the POI compared to the large fusion tags. Since tetramerization is important for the functionality of LacI,[81−83] we investigated the impact of dye labeling on the ability of LacI to form tetramers. Affinity purified, N-terminally His6-tagged LacI-TCO*-AK variants were labeled with sulfo-Cy5-tet and the oligomerization state of the proteins was analyzed based on their mobilities in native polyacrylamide gels. The negatively charged sulfo-Cy5-tet was chosen for labeling to better preserve the overall charge of LacI in native PAGE. As a reference for the oligomerization state of LacI, we used a LacI variant ("LacI-Dim") where the C-terminal tetramerization helix was replaced with the His6 purification tag. Since mutations in the C-terminal tetramerization helix abolish the ability of LacI to tetramerize but do not affect dimerization,[83,84] "LacI-Dim" is expected to move as a dimer in native PAGE. A lower mobility of the dye-labeled LacI variants relative to the "LacI-Dim" standard would therefore indicate that the protein is able to form oligomers consisting of more than two subunits. To verify that the mobility differences of the LacI variants in native PAGE reflect differences in the oligomerization state rather than differences in net charges of the proteins, values for the isoelectric points (pI) of the LacI variants were calculated as described in the Methods section. The pI value for the N terminally His6-tagged and dye-labeled LacI-Y12TCO*-AK and LacI-A312TCO*-AK as well as the nonlabeled, N terminally His6-tagged LacI WT variant was close 6.70. The pI of the C terminally His6-tagged "LacI-Dim" was 6.51. Thus, given the similar pI values for the different LacI variants, the proteins are expected to move under native PAGE conditions (pH 8.3) predominantly based on their oligomerization state. In line with the expectation that the dye-labeled LacI would preserve its ability to tetramerize, the major fluorescent bands of the dye-labeled LacI-Y12TCO*-AK and LacI-A312TCO*-AK variants exhibited a significantly lower mobility compared to the "LacI-Dim" reference protein (Figure 2C). Furthermore, the major fluorescent species in the LacI-Y12TCO*-AK and LacI-A312TCO*-AK samples displayed a mobility close to that of the N-terminally His6-tagged WT LacI (Figure 2C). The analysis also revealed a minor fluorescent species with an intermediate mobility (Figure 2C). Since this minor species was recognized by the LacI specific antibody (Figure 2C), it may represent a LacI trimer as observed in earlier studies.[85]

Though an unambiguous assignment of the major fluorescent LacI bands to tetramer would require a more precise mobility calibration using, for example, a chemically cross-linked LacI tetramer,[85] the significantly lower mobility of the dye-labeled LacI relative to the dimeric "LacI-Dim" indicates that the dye-labeled and TCO*-AK containing LacI can form oligomers consisting of more than two subunits. Moreover, the similar mobilities of the dye-labeled LacI variants and WT LacI indicate that LacI preserves its WT-like folding after dye labeling. Thus, we conclude that the small fluorophore labeling does not grossly perturb the folding and functionality of LacI.

Presence of Additional Fluorescently Labeled Proteins. Though the dye-labeled LacI and OmpC were the major fluorescent species in the in-gel analysis (Figure 2A,B, Figure S11A,B), the analysis also revealed the presence of additional fluorescent molecules (Figure 2D, Figure S11A,B). Since these additional fluorescent proteins were also observed in the recoded strain C321.ΔA.exp (Figure 2D) which lacks endogenous TAG codons, those labeled proteins are unlikely to result from an "off-target" incorporation of the NcAA and its subsequent labeling with the dye The majority of these fluorescent species had a lower molecular weight than the full-length LacI and OmpC (Figure S11A,B). At least some of those lower molecular weight species may therefore be degradation products of the fluorescently labeled LacI or OmpC. Indeed, when the presence of the additional fluorescent proteins was analyzed after dye labeling of affinity purified N-terminally His6-tagged LacI variants, these lower molecular species were more abundant in samples containing the "clickable" LacI compared to WT LacI (Figure S12A,B). However, two

DOI: 10.1021/acssynbio.6b00138
ACS Synth. Biol. XXXX, XXX, XXX−XXX

fluorescent species with molecular weights below 36 kDa and 55 kDa, respectively, were observed in cells grown without NcAA or in the presence of the tetrazine unreactive BocK (Figure S13A,B), indicating that the dye had reacted with endogenous proteins. Though we did not undertake a further characterization of those fluorescent proteins, we note that the 55 kDa species has previously been proposed to represent a dye-PylRS conjugate.[34] However, since we find that the 55 kDa fluorescent species also occurs in the absence of PylRS expression (Figure S14), we doubt that this molecule is a dye-labeled PylRS.

Presence of Endogenous TAG Stop Codons Does Not Increase Spurious Dye Incorporation. The majority of the NcAA incorporation and dye labeling experiments in this study were performed in the UAG-less *E.coli* strain C321.ΔA.exp. However, we envisage situations where the NcAA-based small fluorophore labeling needs to be performed in "native" *E.coli* strains containing the ca. 300 endogenous TAG stop codons. In that case one will anticipate a certain level of the NcAA incorporation at the endogenous TAG with the concomitant spurious dye labeling of the proteome in addition to the labeling of the protein of interest. Such an "off-target" labeling of the host proteome will lead to an increased background fluorescence in cells and thus impair the specific detection of the labeled protein of interest, especially if the latter is present at low levels. We were therefore interested if and to what extent the presence of the endogenous TAG codons increases spurious dye incorporation into the cellular proteome due to the "off-target" incorporation of the NcAA at those codons. Using in-gel fluorescence as readout we therefore compared ATTO647N-tet incoporation into the proteomes of C321.ΔA.exp and a nonrecoded *E.coli* strain BW25993. BW25993 is very similar to the MG1655-derived EcN2 parent strain that was used in the construction of the strain C321.ΔA.exp.[56] Contrary to the expectation that the spurious dye incoporation would increase in the presence of multiple endogenous TAG codons we observed similar levels of "off-target" incorporation of the dye in the C321.ΔA.exp and BW25993 strains in the presence of the $tRNA^{Pyl}$/PylRS pair and the "clickable" NcAA (Figure 2D and 2E). This finding was later confirmed when the specificity of OmpC labeling was compared in BW25993 and C321.ΔA.exp (see below). We therefore discuss the potential causes for this lack of an increased "off-target" dye incorporation in BW25993 in this section. We envision two explanations for the absence of an increased "off-target" labeling of the cellular proteome in the presence of the endogenous amber codons: (i) the endogenous TAG codons are inefficiently decoded by the NcAA-$tRNA^{Pyl}$ or (ii) the $tRNA^{Pyl}$-dependent read-through products are efficiently degraded by *e.g.* the tmRNA-dependent degradation pathway. An inefficient decoding of the endogenous TAG codons by $tRNA^{Pyl}$ may be due to codon context since previous biochemical data indicate a preferred nucleotide context for an efficient decoding of the stop codons by their cognate release factors[86−88] and highlight the importance of the nucleotide immediately 3′ of the stop codon for the release factor decoding.[86−88] Within the preferred codon context the decoding of the stop codons by the release factors is enhanced relative to the suppressor tRNA-dependent read-through.[87] Importantly, while uridine is the preferred nucleotide 3′ to the RF1-decoded endogenous TAG codons in *E.coli* K12,[87] the same uridine was least efficient in promoting the $tRNA^{Pyl}$-dependent decoding of the TAG stop codon.[74,75] Thus, at the "legitimate" TAG stop codons, RF1 may outcompete the suppressor tRNA and in this way restrict the NcAA incorporation at those codons. The idea that RF1 is able to outcompete the suppressor $tRNA^{Pyl}$ at endogenous TAG codons is supported by a recent study of Johnson and co-workers where the $tRNA^{Pyl}$-dependent NcAA incorporation at the endogenous TAG codons was enhanced upon RF1 deletion.[76]

Degradation of the NcAA-containing proteins resulting from the NcAA-$tRNA^{Pyl}$-dependent readthrough of the endogenous TAG codons may also limit the "off-target" incorporation of the NcAA into endogenous proteins. In this scenario, the suppressor tRNA-dependent readthrough of native TAG codons eventually results in the ribosome-nascent chain complex stalling at the 3′-end of the mRNA.[89] This stalling complex is recognized by the transfer-mRNA (tmRNA), leading to the degradation of the NcAA-containing illegitimately extended polypeptide.

In addition to those factors, the low level of the "off-target" NcAA incorporation at the endogenous UAG by $tRNA^{Pyl}$ may be explained by a recent finding that among the three stop codons in *E.coli,* TAG is predominantly found in genes expressed at low levels.[90] Moreover, $tRNA^{Pyl}$ may be mostly sequestered in ribosomal complexes carrying the TAG containing mRNA, leaving a small fraction of it for the decoding of the endogenous amber codons. We note that our observation of similar levels of spurious dye incorporation in the presence or absence of the endogenous TAG codons is in agreement with the observation of Uttamapinant and co-workers[47] where only minimal spurious dye incorporation was seen in the presence of BCN-K when proteins were labeled with tetrazine fluorophores in mammalian cells.

Taken together, we have shown a specific and rapid labeling of the NcAA-containing proteins with tetrazine fluorophores but find that the labeling yields are lower with the more hydrophilic dyes. Furthermore, though the foregoing analysis showed the "clickable" NcAA-containing protein to be the major target of dye incorporation, the analysis also revealed some NcAA-independent "off-target" incorporation of the tetrazine fluorophores, indicating that the fluorescent dyes can react with endogenous molecules.

Extensive Nonspecific Dye Retention Precludes a Microscopy Analysis of the Labeled LacI in Cells. The foregoing in-gel fluorescence analysis indicates that the *in vivo* labeling of LacI with tetrazine fluorophores is largely specific to the "clickable" protein. We therefore proceeded to the analysis of LacI labeling in live cells using fluorescence microscopy. Since in the in-gel analysis the highest labeling yields of LacI had been observed with ATTO647N-tet and Cy5-tet (Figure 2A), those dyes were selected for LacI labeling in the following experiments. Out of the three LacI variants (LacI-Y12NcAA, LacI-Q153NcAA, LacI-A312NcAA) we chose the LacI-Y12NcAA variant for labeling since, despite its lower expression level compared to the LacI-A312NcAA variant, more dye-labeled protein per protein expressed was observed with the LacI-Y12NcAA variant (Figure 1D, Figure S5C,D). The recoded C321.ΔA.exp cells expressing LacI-Y12BCNK or LacI-Y12TCO*-AK were treated with ATTO647N-tet or Cy5-tet, and the fluorescence in the cells was analyzed by microscopy after an extensive washout of the unreacted dye. As a control for any nonspecific dye uptake we used cells expressing WT LacI grown in the presence of a "clickable" NcAA. Cells expressing WT LacI in the presence of a

DOI: 10.1021/acssynbio.6b00138
ACS Synth. Biol. XXXX, XXX, XXX−XXX

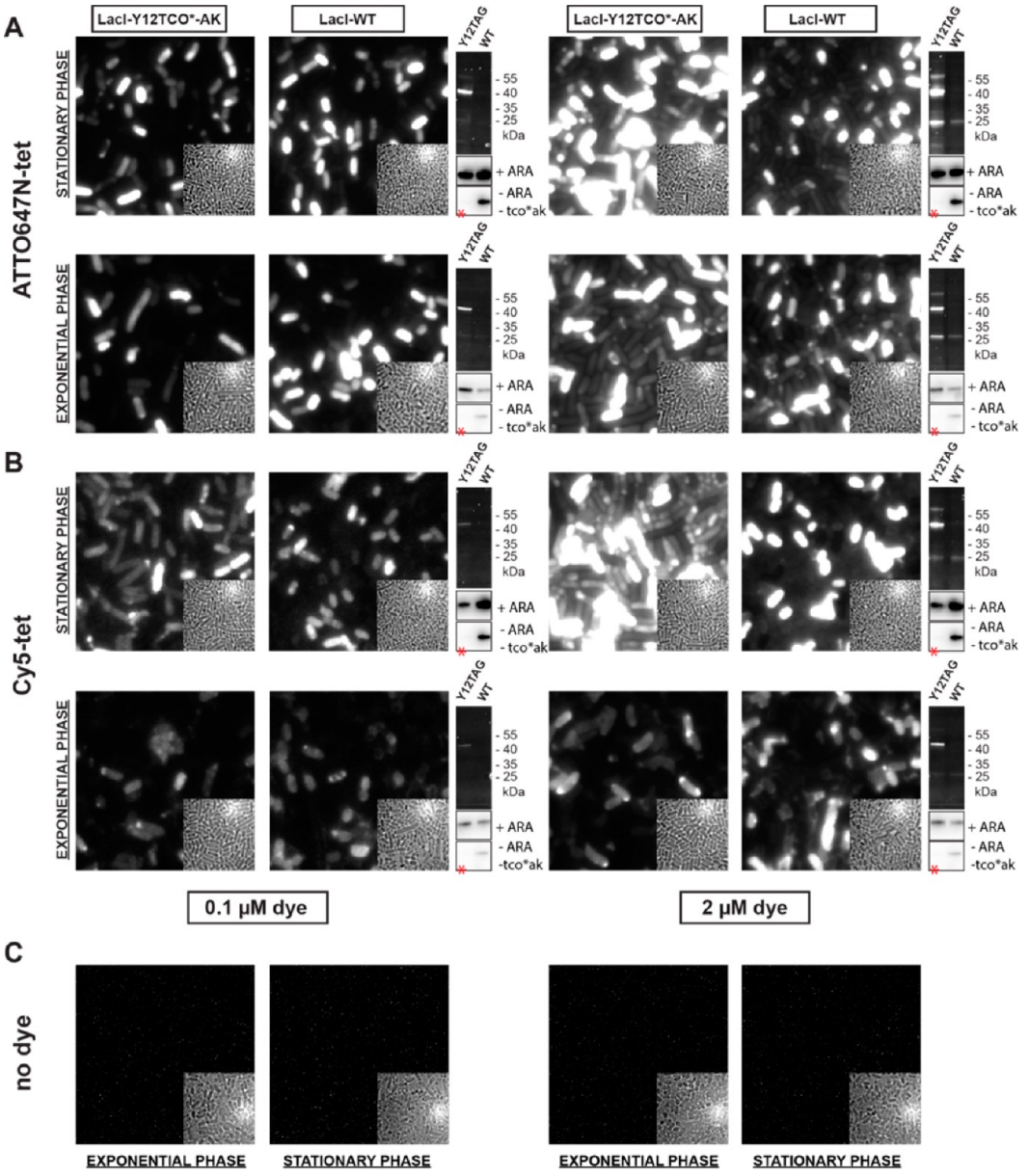

Figure 3. Microscopy imaging of the LacI-Y12TCO*-AK expressing C321.ΔA.exp cells after labeling with tetrazine fluorphores. Cells transformed with pEVOL and pBAD24-LacI-Y12TAG or pBAD24-LacI-WT were grown in the presence of 1 mM TCO*-AK and 0.0002% (LacI-WT) or 0.02% L-arabinose (LacI-Y12TAG) in LB at 37 °C. Cells were harvested at ΔOD600 = 0.6 ("exponential phase") or ΔOD600 = 2.5 ("stationary phase"). After a copious washout of excess TCO*-AK cells were incubated with 0.1 μM or 2 μM ATTO64N-tet (A) or Cy5-tet (B) at 37 °C for 30 min. In panel C dye treatment of the cells was omitted. Cells were imaged on agarose pads at ambient temperature using a 638 nm excitation laser at a beam intensity of 10 W/cm^2 with 50 ms exposure time. EMCCD camera gain was set to 5. The pixel intensities in the fluorescence images from the LacI-Y12TCO*-AK and LacI-WT samples treated at one dye concentration (0.1 μM or 2 μM) were adjusted to the same brightness-contrast scale as described in the Methods section. In panels A and B, dye-labeled cells were analyzed for LacI expression and dye labeling by Western blot and in-gel fluorescence as described in Figure 1. The asterisk-marked Western blot images show LacI expression in controls withdrawn from the main expression cultures before L-arabinose and TCO*-AK addition.

"clickable" NcAA have the advantage of allowing to control for (i) any LacI overexpression-related dye retention while simultaneously controlling for (ii) nonspecific dye retention due to "off-target" incorporation of the NcAA or (iii) a reaction between the dye and traces of the "free" NcAA. Using LacI-NcAA expressed in the presence of a nonclickable NcAA as a control would miss the nonspecific dye incoporation due to the "off-target" incoporation of the NcAA or reaction of the dye with the remaining "free" NcAA. The expression level of WT LacI was adjusted to the level of LacI-NcAA by titrating the concentration of the inducer L-arabinose (Figure S3).

In contrast to the NcAA-specific fluorescence labeling of LacI as observed in the in-gel analysis (Figure 2A) we were unable to detect fluorescently labeled LacI in the cells by microscopy due to the high background fluorescence resulting from the dye treatment (Figure 3A,B, Figure 4A,B, Figure S15,S16). The dye-related background fluorescence markedly exceeded the background fluorescence in cells where dye treatment had been omitted (Figures 3C and 4C). Use of the more highly expressed LacI-A312NcAA variant (Figure 1C) in the in-cell labeling did not yield a LacI-specific fluorescence signal that would be detectable over the high background fluorescence

DOI: 10.1021/acssynbio.6b00138
ACS Synth. Biol. XXXX, XXX, XXX−XXX

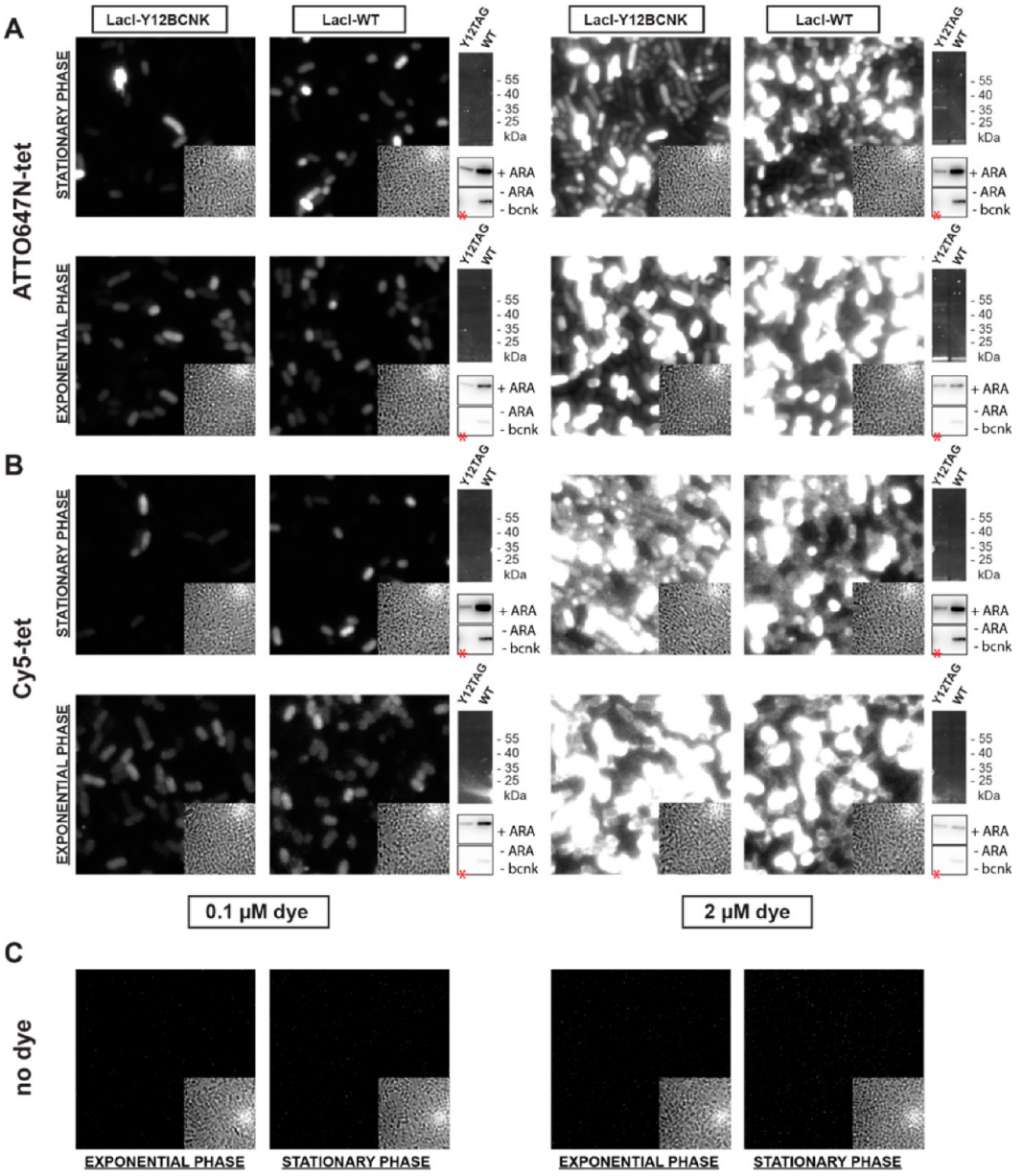

Figure 4. Microscopy imaging of the LacI-Y12BCNK expressing C321.ΔA.exp cells after labeling with tetrazine fluorophores. LacI-Y12BCNK expression and dye labeling were performed as described in Figure 3. (A) Labeling with ATTO64N-tet. (B) labeling with Cy5-tet. (C) Cells without dye treatment Cells were imaged on agarose pads at ambient temperature for dye fluorescence using a 638 nm excitation laser at a beam intensity of 10 W/cm^2 with 50 ms exposure time. EMCCD camera gain was set to 5. The pixel intensities in the fluorescence images from the LacI-Y12BCNK and LacI-WT samples treated at one dye concentration (0.1 μM or 2 μM) were adjusted to the same brightness-contrast scale as described in the Methods section. In-gel fluorescence and Western blot analysis in panels A and B were performed as described in Figure 1. The asterisk-marked Western blot images show LacI expression in controls withdrawn from the main expression cultures before L-arabinose and BCNK addition.

(Figure S17). Strong dye fluorescence was also observed in (i) cells grown in the absence of the NcAA and in (ii) cells expressing the "unclickable" LacI-BocK (Figure S18). The high fluorescence background observed in cells grown without any NcAA rules out the nonspecific dye retention as a result of (i) an incorporation of the NcAA into the cellular proteome through an occasional misreading of sense codons by tRNA^{Pyl} or (ii) an insufficient removal of the NcAA prior to the dye treatment as suggested based on protein labeling in eukaryotic cells.[47,91] Though the high background fluorescence precluded observation of the fluorescently labeled LacI by microscopy, in gel analysis confirmed the presence of a fluorescently labeled LacI in the LacI-Y12TCO*-AK expressing cells (Figure 3A,B). In the LacI-Y12BCNK expressing cells, fluorescently labeled LacI was only seen in cells treated with 2 μM ATTO647N-tet (Figure 4B). Western blot analysis confirmed the expression of LacI in all microscopy samples (Figures 3 and 4). Thus, though LacI can be conjugated with the membrane permeable tetrazine dyes in intact cells, we could not detect this labeled LacI by microscopy due to the high nonspecific binding of the dyes to intracellular components and the resulting high background fluorescence. We sought to alleviate the nonspecific dye binding by using sulfo-Cy5-tet, reasoning that the lower labeling yield with it in intact cells (Figure 2A) may be compensated by its lesser intracellular binding due to the presence of the sulfo groups, allowing a specific detection of the fluorescent LacI

DOI: 10.1021/acssynbio.6b00138
ACS Synth. Biol. XXXX, XXX, XXX−XXX

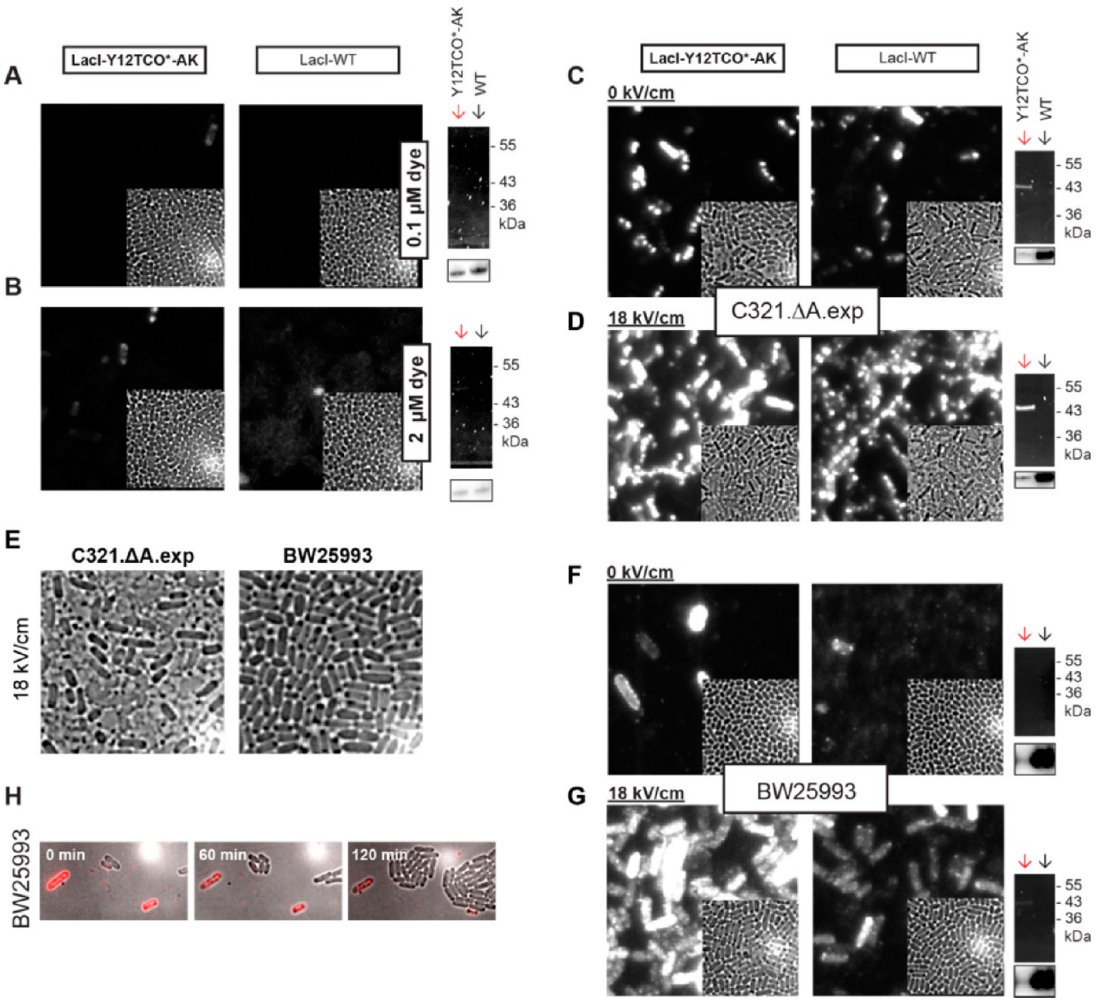

Figure 5. LacI-Y12TCO*-AK labeling with sulfo-Cy5-tetrazine. C321.ΔA.exp cells transformed with pEVOL and pBAD24-LacI-Y12TAG or pBAD24-LacI-WT were grown in LB at 37 °C in the presence of 1 mM TCO*-AK and harvested at ΔOD600 = 0.6. Cells were treated with sulfo-Cy5-tet at 0.1 μM (A) or 2 μM (B) as described for Cy5-tet in Figure 3. Cells were imaged on agarose pads at ambient temperature using a 638 nm excitation laser at a beam intensity of 10 W/cm^2 with 50 ms exposure time. EMCCD camera gain was set to 5. The brightness-contrast of the fluorescence images was adjusted to the same scale as in the fluorescence images of cells treated with 0.1 μM or 2 μM Cy5-tet in Figure 3. (C−H) Electroporation of sulfo-Cy5-tet. C321.ΔA.exp (C,D) cells expressing LacI-Y12TCO*-AK or LacI-WT were grown as in panel A and harvested at ΔOD600 = 0.8. The cells were made electrocompetent by repeated washes with 10% glycerol and electroporated in the presence of 2 μM sulfo-Cy5-tet. Cells were recovered in LB at 37 °C for 1.5 h followed by a 12 h washout of the dye. Cells were imaged on agarose pads using a 638 nm excitation laser at a beam intensity of 830 W/cm^2 with 50 ms exposure time. EMCCD camera gain was set to 30. (E) Effect of electroporation in C321.ΔA.exp and in BW25993. Brightfield images of the cells electroporated at 18 kV/cm field strenght are shown. (F,G). Electroporation of sulfo-Cy5-tet in BW25993. Treatment of the cells was as in panels C and D. (H) BW25993 cells from panel G were incubated at 4° for one day and then imaged on agarose pads supplemented with 1×RPMI amino acids and 0.15 μg/mL D-biotin. Cell growth was monitored at 37 °C.

over the background. However, the use of sulfo-Cy5-tet did not result in a LacI specific signal in the LacI-Y12TCO*-AK expressing cells relative to the controls (Figure 5A,B, Figure S19). Efforts to facilitate the intake of sulfo-Cy5-tet in C321.ΔA.exp by electroporation[23,92] did not lead to a LacI-specific fluorescence signal in the LacI-Y12TCO*-AK expressing cells relative to the control (Figure 5C,D) and the electroporation was detrimental to the cells (Figure 5E). Encouragingly, electroporation of sulfo-Cy5-tet in BW25993 led to an increased fluorescence in the LacI-Y12TCO*-AK expressing cells compared to the control (Figure 5F and 5G), indicating that when sulfo-Cy5-tet is used the labeled LacI can be detected over the background. However, the fluorescent LacI-Y12TCO*-AK containing cells did not resume growth under conditions in which the nonfluorescent cells were able to divide (Figure 5H), apparently due to the detrimental effect of electroporation. Though the electroporation did not yield LacI specific labeling in living cells, we think that an optimization of the electroporation conditions (e.g., incubation times, growth medium, field strength) may make electroporation a viable means of dye delivery since molecules as large as proteins can be delivered into *E.coli* while still retaining cell viability[93]

Search for the Factors Contributing to the Nonspecific Fluorescence Incorporation. Since our in-gel analysis had revealed some "off-target" protein labeling (Figure 2E,D Figure S12 and S13), we analyzed the contribution of these spuriously labeled fluorescent species to the total fluorescence signal from cell-extracted material. We found that the additional bands contributed roughly 70% of the total in-gel fluorescence when the LacI-Y12TCO*-AK bearing exponential phase cells were treated with 0.1 μM ATTO647N-tet (Figure S20). This substantial spurious fluorescence incorporation partly explains

DOI: 10.1021/acssynbio.6b00138
ACS Synth. Biol. XXXX, XXX, XXX−XXX

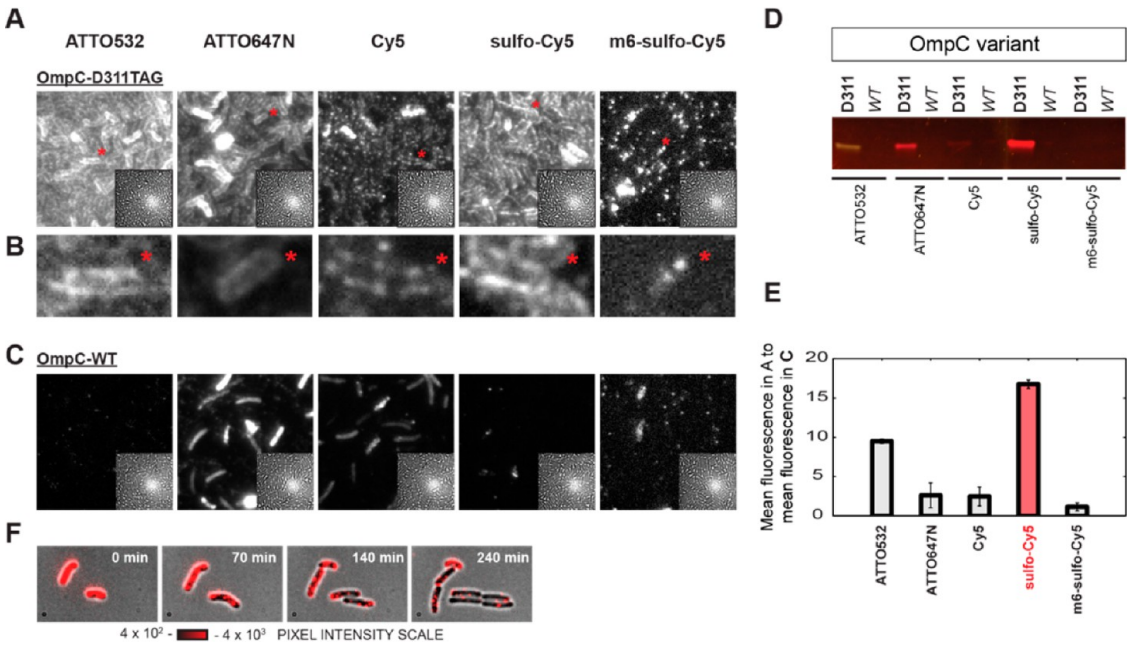

Figure 6. Labeling of OmpC with tetrazine fluorophores. C321.ΔA.exp cells transformed with pEVOLV and pBAD24-OmpC-D311TAG or pBAD24-OmpC-WT were grown in the presence of 1 mM TCO*-AK at 30 °C in M9/0.7% glycerol supplemented with amino acids and 15% LB. Cells were harvested at ΔOD600 = 0.5−0.7, repeatedly washed with growth medium over 2.5 h and incubated with 10 nM of one of the tetrazine dyes for 20 min at 37 °C. Cells were washed with the growth medium over 2.5 h and imaged on agarose pads using a 514 nm (for ATTO532-tet) or 638 nm excitation laser. EMCCD camera gain was set to 50 and camera exposure was 50 ms. (A) Cells expressing OmpC-D311TCO*-AK. (B) A magnified view of a fluorescently labeled cell (marked with asterisk) from panel A. (C) Cells expressing WT OmpC. (D) In-gel fluorescence analysis of OmpC labeling in the microscopy samples from A and C ("D311", OmpC-D311TCO*-AK; "WT", OmpC-WT). (E) Ratios of the mean pixel intensities from the images in panel A to the mean pixel intensities in panel C. (F) Growth of the sulfo-Cy5-treated C321.ΔA.exp cells. Cells were grown and labeled with 10 nM sulfo-Cy5-tet as described above. Cells were incubated at 4 °C for 48 h and imaged on agarose pads supplemented with 1 × RPMI amino acids and 0.15 μg/mL D-biotin at 37 °C.

the high nonspecific fluorescence retention in those samples. However, in the stationary-phase derived cells treated with 0.1 μM ATTO647N-tet, LacI was the main fluorescent species, accounting for 73% of the total in-gel fluorescence (Figure S20). Thus, a covalent labeling of those additional proteins with the dye cannot fully account for the nonspecific dye retention in all situations.

Though our finding that the occurrence of the 55 kDa spurious fluorescent species is unrelated to the expression of PylRS (Figure S14) does not support the idea of a direct reaction between PylRS and the tetrazine fluorophores, at least in the absence of the NcAA, we analyzed whether the expression of one or both components of the $tRNA^{Pyl}$/PylRS pair indirectly affects the nonspecific dye retention. The retention of ATTO647N-tet was analyzed in C321.ΔA.exp cells harboring (i) a PylRS-free derivative of pEVOL ("pEVOL-ΔPylRS") or (ii) the original pEVOL containing one constitutively expressed and one arabinose-inducible copy of PylRS. Dye retention was analyzed in cells grown in the absence of NcAA or in cells grown in the presence of 1 mM BCNK or TCO*-AK. Curiously, microscopy analysis revealed that the expression of $tRNA^{Pyl}$ alone, independently of the expression of PylRS, led to a significantly increased dye retention compared to controls devoid of $tRNA^{Pyl}$ and PylRS (Figure S21A). Moreover, this $tRNA^{Pyl}$-dependent dye retention was independent of NcAA addition to the expression culture (Figure S21A). Expression of PylRS, either from a constitutive or arabinose inducible promoter, did not make a further contribution to the dye retention (Figure S21A). In line with these findings, an in-gel analysis of the microscopy samples expressing $tRNA^{Pyl}$ alone or in combination with PylRS revealed a similar pattern of fluorescent proteins (Figure S21B). In contrast, significantly less fluorescence was observed in the sample devoid of $tRNA^{Pyl}$ regardless of the presence of the NcAA (Figure S21A,B). It thus seems that $tRNA^{Pyl}$ alone contributes to the increased nonspecific dye retention. Since the known reaction specificity of the tetrazines makes it hard to conceive how a $tRNA^{Pyl}$ lacking the NcAA could form a covalent adduct with the tetrazine dyes, the alternative explanation is that the $tRNA^{Pyl}$-dependent dye retention is an indirect effect of the overexpression of $tRNA^{Pyl}$. The influence of $tRNA^{Pyl}$ on the nonspecific retention of tetrazine fluorophores has earlier been observed by Uttamapinant and co-workers though the authors interpret this effect as due to the reaction of the tetrazine dyes with BCNK attached to $tRNA^{Pyl}$.[47]

We conclude the LacI labeling section by noting that though LacI could be conjugated with tetrazine fluorophores in intact cells, an *in vivo* observation of the labeled LacI was complicated due to the high fluorescence background when membrane permeable dyes were used. Use of the more hydrophilic sulfo-Cy5-tet on the other hand was complicated by its poor membrane permeability.

Labeling of Extracellular Proteins. We next turned to the labeling of proteins exposed on the outer membrane of *E.coli*, where the restricted membrane permeability and nonspecific binding of the dyes to intracellular components do not obstruct the labeling and detection of the fluorescent protein. As a model protein for the NcAA-based small fluorophore labeling we used outer membrane porin OmpC, a homotrimeric β-

DOI: 10.1021/acssynbio.6b00138
ACS Synth. Biol. XXXX, XXX, XXX−XXX

barrel protein consisting of 16 transmembrane β-sheets that are connected by eight external and seven internal loops.[68] OmpC (along with OmpF and PhoE) is one of the most abundant outer membrane proteins in *E.coli* and is involved in the control of cellular osmolarity and the uptake of nutrients and antibiotics.[67,80,94] The pore in OmpC allows passage of hydrophilic molecules of up to 600 Da[67] with a slight preference for cationic compounds.[80,94] OmpC is also known to serve as a receptor for bacteriophages[80] and colicins[95] and has been used as a target for a site-specific incoporation of azidohomoalanine at methionine codons for a cell surface labeling with biotin.[96]

Fluorescently Labeled OmpC Can Be Specifically Detected in Live Cells. We incorporated TCO*-AK into OmpC at position 311 in the extracellular loop 7 (Figure S1) in *E.coli* C321.ΔA.exp and labeled the OmpC-D311TCO*-AK variant with the tetrazine dyes ATTO532-tet, ATTO647N-tet, Cy5-tet, sulfo-Cy5-tet, and m6-sulfo-Cy5-tet. After a 20 min labeling at a 10 nM dye concentration, microscopy analysis revealed a membrane-localized fluorescence in the OmpC-TCO*-AK expressing cells with all dyes except for m6-sulfo-Cy5 (Figure 6A,B). With the hydrophilic dyes ATTO532-tet and sulfo-Cy5-tet little fluorescence was observed in cells expressing OmpC from the WT construct in the presence of TCO*-AK (Figure 6C, Figure S22A) or in cells expressing OmpC from the TAG-containing construct in the presence of the "unclickable" eBocK (Figure S22A). This specific labeling of the "clickable" protein in the case of OmpC is in clear contrast with the lack of specificity in LacI labeling and recapitulates the specificity of outer membrane protein labeling as reported for eukaryotic cells.[35,38] In-gel analysis confirmed the specificity of the "clickable" OmpC labeling (Figure 6D, Figure S22B,C). In contrast to ATTO532-tet and sulfo-Cy5-tet, use of the more hydrophobic (Table 1) and more cell permeable (Figure 2A) dyes ATTO647N-tet and Cy5-tet led to a noticeable fluorescence retention in the WT OmpC expressing controls (Figure 6C). However, this nonspecific fluorescence was not localized to the membranes but was distributed over the entire cell (Figure 6C). As the highest OmpC-specific signal over the background fluorescence was seen when OmpC was labeled with sulfo-Cy5-tet (Figure 6E), this dye was selected for the subsequent experiments. The sulfo-Cy5-tet treated OmpC-D311TCO*-AK expressing C321.ΔA.exp cells were able to divide when cultivated on agarose pads (Figure 6F), indicating that the labeling protocol is compatible with cell viability. Preservation of cell viability after dye labeling was later confirmed by experiments where sulfo-Cy5-treated OmpC-D311TCO*-AK expressing C321.ΔA.cells were cultivated in a microfluidic device (see the section on single particle tracking of OmpC). The level of the sulfo-Cy5-tet labeled OmpC-D311TCO*-AK did not markedly decrease over a period from 6 h to 5 days when the labeled OmpC bearing cells were incubated in M9 medium at an ambient temperature (Figure S23) and a clear membrane-localized fluorescence signal was observed on the cells harvested from the 5 day time point (Figure S24). This result indicates that even after an extended *in vivo* incubation the fluorescently labeled OmpC is present at levels sufficient for microscopy analysis. Reverting to the issue of the nonspecific dye binding in LacI labeling with sulfo-Cy5-tet, we noted that at the 10 nm sulfo-Cy5-tet concentration used for OmpC labeling (10-fold lower concentration compared to the lowest concentration of 0.1 μM sulfo-Cy5-tet used in LacI labeling) the nonspecific dye binding in LacI-Y12TCO*-AK expressing cells was negligible compared to the OmpC-D311TCO*-AK specific fluorescence and was close to the background fluorescence in the OmpC-WT expressing cells (Figure S25).

Dye-Labeled OmpC Is Localized on the Membrane. Though the fluorescence in the OmpC-D311TCO*-AK expressing cells was localized in membrane-proximal regions after dye treatment, the limited spatial resolution of the microscopy setup does not unambigously distinguish if the labeled OmpC is localized in the outer membrane or in, for example, the periplasm. We therefore analyzed the cellular localization of the fluorescently labeled OmpC by proteinase K treatment since OmpC is known to be cleaved by proteinase K at a surface exposed region between residues 155−169.[97] A proteinase K cleavage of the fluorescently labeled OmpC would thus indicate that the protein is localized in the outer membrane. Consistent with this, when material from proteinase K treated sulfo-Cy5-OmpC bearing cells was analyzed by SDS-PAGE, a lower molecular weight fluorescent species was observed in addition to the full-length fluorescent OmpC (Figure S26A). The size of the lower molecular species (Figure S26A) is close to the size of the C-terminal OmpC cleavage product (21 kDa) as observed by Morona and colleagues.[97] Only full-length sulfo-Cy5-OmpC (molecular weight 38.3 kDa) was observed when proteinase K treatment was omitted (Figure S26A). In agreement with the in-gel analysis, proteinase K treatment reduced the membrane-bound fluorescence on the fluorescently labeled OmpC bearing cells (Figure S26B), indicating that the cleavage fragment is at least partially released from the outer membrane. Together, these data indicate that the fluorescently labeled OmpC is accessible to the proteinase and is therefore localized in the outer membrane.

Dye Labeling Preserves OmpC Folding. To analyze the impact of the dye labeling on the folding and oligomerization of OmpC, we made use of the fact that the correctly folded outer membrane porins, including OmpC, are known to retain their oligomeric state in denaturing polyacrylamide gel electrophoresis when the heat treatment of the sample prior to SDS-PAGE is omitted.[98,99] We therefore monitored the mobility of the sulfo-Cy5-tet labeled OmpC in denaturing PAGE in the presence and absence of heat treatment. When the heat treatment was omitted the dye-labeled OmpC (monomeric molecular weight 38.3 kDa of the mature OmpC after cleavage of the 21 amino acid N-terminal signal peptide) exhibited an apparent molecular weight between 95 and 130 kDa (Figure S27), thus close to the nominal molecular weight of 114 kDa of an OmpC trimer. After the sample was heated to 95 °C a single fluorescent species with a molecular weight close to 40 kDa was observed (Figure S27), in agreement with the mobility of an OmpC monomer. On the basis of the above observations we conclude that the NcAA incorporation and dye labeling do not interfere with the oligomerization of OmpC.

Optimizing TCO-AK Washout.* One important consideration in the NcAA-based protein labeling is the efficient removal of the NcAA prior to dye labeling. We therefore tested different washout schemes with the aim of removing the NcAA from the cells using a minimal number of washing steps. Initially, we tried to remove the NcAA by washing the cells over 1 h with a solution consisting of M9 salts and 0.8% glycerol. However, this NcAA washout protocol resulted in a notable nonspecific fluorescence retention in membrane-proximal regions when the control cells expressing WT OmpC in the presence of 1 mM TCO*-AK were incubated with 10 nM sulfo-

DOI: 10.1021/acssynbio.6b00138
ACS Synth. Biol. XXXX, XXX, XXX−XXX

Cy5-tet (Figure S28A). This nonspecific dye retention was specific to a "clickable" NcAA in the expression culture as little nonspecific dye fluorescence was seen in the OmpC-D311BocK expressing cells (Figure S28A). An in-gel fluorescence analysis of the labeling samples showed a fluorescent protein only in the OmpC-D311TCO*-AK containing sample (Figure S28B), indicating that the nonspecific fluorescence retention is not caused by a misincorporation of TCO*-AK into the WT variant of OmpC or another membrane protein. On the basis of the known role of OmpC in the intake of exogenous small molecules[94] we speculate that the nonspecific dye retention results from an entrapment of TCO*-AK in the periplasm and its subsequent reaction with the tetrazine dye the intake of which may be facilitated by the porin OmpC itself. This putative entrapment of the NcAA is reversible as little nonspecific fluorescence was observed in the cells when the NcAA washout was extended to 12 h (Figure S28C). Though the prolonged NcAA washout eliminated the nonspecific dye binding, such a long washing procedure is undesirable for physiological studies. However, experiments done when the manuscript was in submission showed that the NcAA washout procedure could be shortened to 1 h when rpmi amino acids and 15% LB were included in the washing solution (Figure S29). This improved NcAA removal in a more nutrient-rich medium suggests that the metabolic state of the cell is an important factor for removing the excess labeling components from the cell. Provided that the NcAA had been efficiently removed prior to dye labeling, removal of sulfo-Cy5-tet could be achieved by two 30 min washing steps in the rpmi amino acid and LB supplemented medium (Figure S30). Though the exact washing conditions may be specific to a given protein and cell line, we have noticed that a prolonged washout procedure in a medium that allows cell growth reduces OmpC fluorescence, probably because the fluorescent OmpC is diluted when cells divide during the washout (Figure S31).

NcAA Incorporation at Endogenous TAG Codons Is Negligible. Having established the conditions for specific labeling of OmpC and the removal of the nonspecifically bound dye in the recoded strain C321.ΔA.exp, we next analyzed the specificity of OmpC labeling with sulfo-Cy5-tet in the presence of endogenous TAG stop codons. Though our in-gel fluorescence analysis indicated the absence of a noticeable spurious dye incorporation into the cellular proteome in a nonrecoded *E.coli* strain during the intracellular labeling experiments, we also tested for nonspecific dye retention in OmpC labeling. We therefore expressed OmpC-TCO*-AK in the nonrecoded strain BW25993 in parallel with the recoded C321.ΔA.exp strain and treated the cells with 10 nM sulfo-Cy5-tet. In line with our previous results with intracellular labeling the fluorescence incorporation in the nonrecoded BW25993 strain in the absence of the tetrazine-reactive OmpC did not exceed the level observed in the recoded strain (Figure 7A–D). We thus conclude that "off-target" incorporation of the NcAA at the endogenous TAG codons is negligible with regard to the membrane proteome of *E.coli* at least in the presence of an excess of the TAG containing transcript. Overall, the low level of spurious dye incorporation in OmpC labeling independently of the presence of endogenous TAG codons supports our previous conclusion that NcAA incorporation and the ensuing dye labeling are specific and that the nonspecific dye retention during intracellular labeling is rather related to interactions of the lipophilic tetrazine dyes with cellular components.

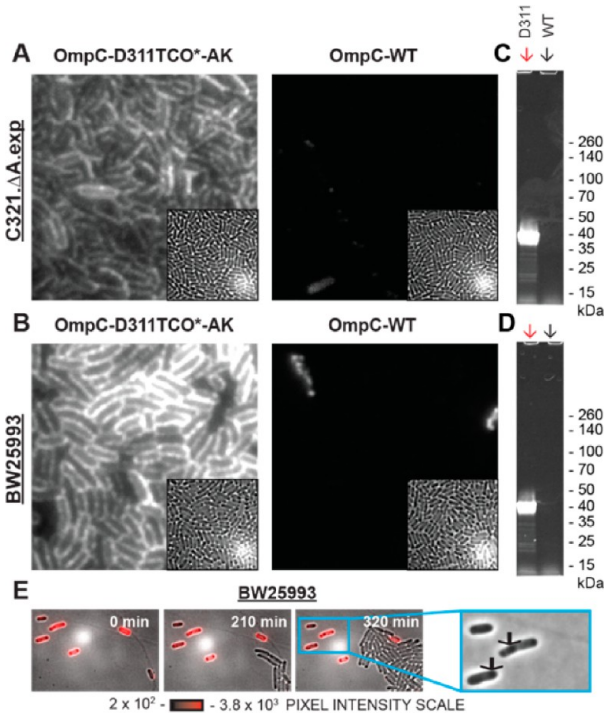

Figure 7. Dye labeling of OmpC in BW25993 and C321.ΔA.exp. C321.ΔA.exp (A) or BW25993 (B) cells transformed with pEVOL and pBAD24-OmpC-D311TAG or pBAD24-OmpC-WT were grown in the presence of 1 mM TCO*-AK at 30 °C in M9/0.7% glycerol supplemented with amino acids and 15% LB. After an extensive washout of excess TCO*-AK with growth medium, cells were incubated with 10 nM sulfo-Cy5-tet for 20 min at 37 °C and imaged on agarose pads using a 638 nm excitation laser at a beam intensity of 50 W/cm^2 with 50 ms camera exposure time. EMCCD camera gain was 50. (C and D) In-gel fluorescence analysis of the labeling products from panels A and B, respectively. (E) Sulfo-Cy5-tet labeled OmpC-TCO*-AK expressing BW25993 cells from panel B were incubated at 4 °C for 48 h and imaged on agarose pads supplemented with 1 × RPMI amino acids and 0.15 μg/mL D-biotin at 37 °C. Blue rectangle denotes a phase contrast image of the fluorescent cells in panel E. The inclusion bodies are denoted by arrows.

Protein Expression from the TAG-Containing OmpC Construct Is Toxic in BW25993. Though we did not observe more spurious protein labeling in the nonrecoded strain BW25993, the dye-labeled-OmpC bearing RF1$^+$ BW25993 cells did not resume growth when cultivated on agarose pads (Figure 7E, Figure S32A), in contrast to the situation in C321.ΔA.exp (Figure 6F, Figure S32B). Such growth impairment may be caused by the expression of a truncated and probably misfolded OmpC from the TAG-containing construct when RF1 competes with tRNA^{Pyl} in TAG decoding. In agreement with this, microscopy analysis revealed dense particles in BW25993 cells expressing OmpC from the TAG-containing construct (Figure 7E, Figure S32A) that may represent inclusion bodies of the truncated OmpC. Those particles are absent from the RF1$^-$ C321 cells (Figure 6F, Figure S32B). An optimization of the expression and incubation conditions may still yield viable fluorescent cells in the presence of RF1. An indication of a possible optimization is the difference in growth rate response of the TAG-containing constructs in different media (Figure S33). There are however conditions (Figures 6 and 7) where the presents of RF1 leads to toxic effects due to truncated proteins. We therefore conclude that usefulness of the

DOI: 10.1021/acssynbio.6b00138
ACS Synth. Biol. XXXX, XXX, XXX–XXX

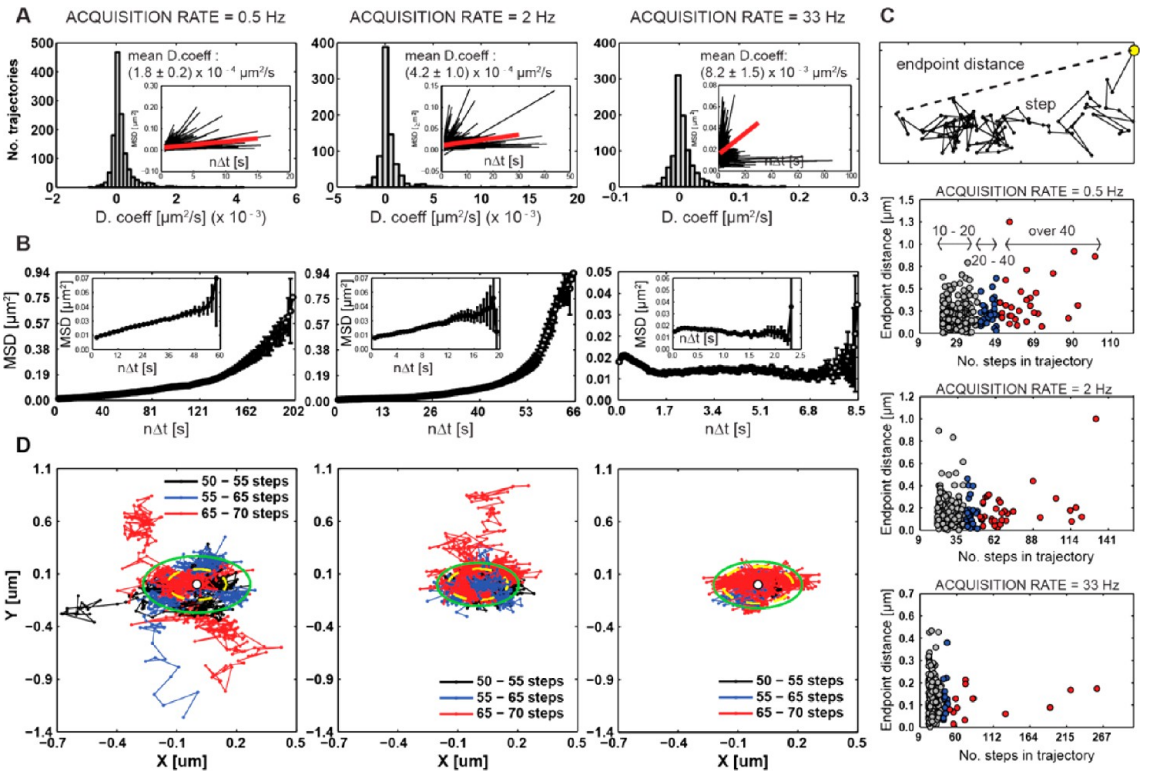

Figure 8. Single particle tracking of Cy5-labeled OmpC in *E.coli* strain C321.ΔA.exp. Sulfo-Cy5-tet treated OmpC-D311TCO*-AK expressing cells were loaded into the traps of a microfluidic device by gravity flow. The device contains 51 cell traps with dimensions of 40 × 40 × 0.9 μm^3. The cells were allowed to grow into monolayers at 37 °C for approximately 7 h with a constant replenishment of fresh growth medium and removal of waste. The movement of Cy5-labeled OmpC was tracked at 37 °C using a 638 nm excitation laser at a beam power of 290 to 660 W/cm^2 at EMCCD camera frame rates of 2 Hz (6 traps) or 0.5 Hz (11 traps) with a total of 200 frames. EMCCD camera and laser exposure times were 150 ms for the 2 Hz and 200 ms for the 0.5 Hz frame rate set. For the 33 Hz data set time-lapse photography images were recorded at a 30 ms camera exposure time with no interval between the exposures. EMCCD camera gain was set to 300. At the beginning and end of the tracking, phase-contrast and brightfield images of the traps were recorded for cell segmentation. During trajectory building the positions of OmpC are mapped to the internal cell coordinates generated during segmentation. The minimal number of steps in a trajectory was set to 10 during trajectory construction. (A) Distribution of OmpC diffusion coefficients estimated by a linear regression of the msd versus time curves of individual trajectories. Points up to $^1/_3$ of the maximal time-lag of a trajectory were used for the regression. The insets show an overlay of the regression lines to individual mean-squared displacement (msd) curves (in black) and an average over all regression lines (in red). (B) The msd versus time curves of OmpC diffusion. The msd values were calculated from the *X*, *Y* positions of the particles. Mean msd values for each time-lag are plotted versus time-lag $n \cdot \Delta t$, where n is the number of steps and Δt is the interval between camera exposures. The insets show a zoom of the msd vs time-curves up to $^1/_3$ of the maximal time-lag over all trajectories in a data set. (C) Scatter plots of trajectory end point distances versus trajectory length (in steps). Color-coding of trajectory length ranges is indicated on the figure. (D) Overlay of individual single particle trajectories of OmpC with lengths from 50 to 70 steps plotted with a color-coding for each trajectory length range (indicated on the figure). The yellow broken circle denotes a region with a radius equal to the mean localization error. The green circle denotes a region with a radius equal to the particle displacement d at the minimal time-lag $n_{min} \cdot \Delta t$ (where n_{min} = 50 is the minimal trajectory length in steps) assuming a "normal" Brownian diffusion according to $d = (2Dn\Delta t)^{1/2}$ with a diffusion coefficient D as estimated from the msd vs time curves in A.

C321.ΔA. exp strain for the NcAA incorporation experiments partly lies in the absence of RF1.

An OmpC Fluorescent Protein Fusion Is Toxic to the Cells. In the OmpC single particle tracking experiments described in the next section, our ambition was to compare the performances of a small fluorophore labeled OmpC and fusion-tagged OmpC. To this end, we cloned the photoconvertible fluorescent protein mEos2[100] into the extracellular loop 7 of OmpC. Loop 7 of OmpC has previously been used for the insertion of exogenous peptide sequences into OmpC. We avoided placing mEos2 to either the N- or C-terminus of OmpC for the following reasons: (i) fusion of mEos2 to the signal sequence containing N-terminus of OmpC[101] may interfere with the SecYEG-dependent translocation[102] of OmpC through the plasma membrane and (ii) in a C-terminal fusion mEos will be facing the periplasm where the oxidizing environment would affect the folding of mEos2 because of the formation of interchain disulfide bridges with other proteins or mEos2 folding intermediates that inhibit the chromophore maturation.[103,104] Unfortunately, expression of the OmpC-mEos2 "sandwich" fusion was detrimental to cells in both the recoded C321.ΔA.exp and the nonrecoded BW25993 strains (Figures S34 and S35). Though mEos2 fluorescence could be observed in membrane-proximal regions in the cells (Figures S34 and S35), the OmpC-mEos2 expressing cells appeared severely damaged (Figures S34 and S35). The negative effect of installing mEos2 into OmpC is in agreement with the results of Xu and Lee in which the insertion of longer poly(His_6) sequences into loop7 severely decreased the expression level of the fusion protein.[69] Since the functionality of OmpC is not necessary for cell viability (as evidenced by the viability of OmpC deletion strains),[105] the marked negative effect of the OmpC-mEos2 expression is likely not due to the loss of function of OmpC but is rather related to OmpC-mEos2

DOI: 10.1021/acssynbio.6b00138
ACS Synth. Biol. XXXX, XXX, XXX−XXX

Table 2. OmpC Diffusion Coefficients and Particle Tracking Parameters[a]

camera aquisition rate (Hz)	diffusion coefficient ($\mu m^2/s$)	localization error (μm)	mean single step size (μm)
0.5	$(1.8 \pm 0.2) \times 10^{-4}$	$(7.3 \pm 1.4) \times 10^{-2}$	$(9.6 \pm 0.4) \times 10^{-2}$
2	$(4.2 \pm 1.0) \times 10^{-4}$	$(7.4 \pm 1.4) \times 10^{-2}$	$(9.4 \pm 0.5) \times 10^{-2}$
33	$(8.2 \pm 1.5) \times 10^{-3}$	$(8.8 \pm 1.5) \times 10^{-2}$	$(11.2 \pm 0.5) \times 10^{-2}$

[a]Diffusion coefficients and localization errors were calculated from the slopes and offsets, respectively, of the regression lines to the msd *versus* time curves of individual single particle trajectories according to msd = $4Dt_{lag} + 2\sigma_{xy}^2$ (D, diffusion coefficient; t_{lag}, time-lag; σ_{xy}, localization error).[138] The mean single step size was calculated as average over all single step displacements from all trajectories obtained at a particular camera acquisition rate. The error estimates of the parameters are given as margins of error (me) at a 95% confidence level according to me = $1.96 \times \text{std}/(N)^{1/2}$ where std is the standard deviation and N the number of msd curves.

interfering with an essential cellular process. For instance, the OmpC-mEos2 fusion protein may not be recognized by the BAM outer membrane folding complex, leading to the accumulation of a misfolded OmpC-mEos2 in the periplasm and an eventual cell death.[106,107] However, we envisage that a more extensive screen for fluorescent protein insertion sites[108] in OmpC may yield fluorescent fusions that are compatible with cell viability.

OmpC Diffusion Is Restricted in E.coli Outer Membrane. In the foregoing experiments we had established a protocol for an OmpC-specific small-molecule labeling in live cells. We went on to apply this protocol to the study of the diffusion of OmpC in its native environment by single particle tracking to harness the advantages of small synthetic fluorophores in terms of increased photostability and lesser interference with the functionality of the POI.

For single particle tracking of OmpC in the outer membrane, C321.ΔA.exp cells containing sulfo-Cy5-tet labeled OmpC were grown from individual cells into microcolonies in the traps of a microfluidic chip (Figure S36A,B). By growth the fluorescent OmpC molecules are diluted to 0.6 ± 0.16 fluorescent molecules per cell (mean fluorophore density over three experiments) at the beginning of image acquisition, making the surface density sufficiently low (Figure S36C−F) for single particle tracking.[109] In the sulfo-Cy5-tet treated WT OmpC expressing control cells only traces of fluorescence could be observed (Figure S37A), confirming that the fluorescence in the OmpC-D311TCO*-AK (Figure S37B) expressing cells is not caused by nonspecific dye binding. This specific fluorescence incorporation was confirmed by an in-gel analysis of material from the microscopy samples (Figure S37C,D). Since membrane proteins have been suggested to display different modes of lateral diffusion ranging from "confined" to "normal Brownian" each with its own characteristic diffusion parameters[4,110−113] we followed the movement of the Cy5-labeled OmpC at camera acquisition rates of 0.5, 2, and 33 Hz to decrease the likelihood of missing a particular mode of diffusion due to time-averaging or undesampling of the trajectories.[114] Though the limited lateral movement of OmpC observed in our experiments (see below) may warrant sampling rates below 0.5 Hz to reveal longer displacements of OmpC, the occasional movements of the cells in the traps would have compromised trajectory building at acquisition rates lower than 0.5 Hz. To filter out false positives during trajectory building we accepted trajectories consisting of minimally 10 steps. Using this cutoff value we collected 800−1300 single particle trajectories per experiment (0.16−0.4 trajectories per *E.coli* cell). The mean trajectory lengths for OmpC were close to 20 steps per trajectory with approximately 25% of trajectories exceeding this value (Figure S38A). The longest trajectories consisted of 101, 132, and 258 steps for the 0.5, 2, and 33 Hz data sets, respectively. These trajectory lengths exceed those regularly observed in single particle tracking experiments with fluorescent protein fusions,[57,113,115] emphasizing the usefulness of the NcAA-based small fluorophore labeling protocol for single molecule experiments.

Diffusion coefficients for OmpC assuming a "normal" diffusion mode were estimated from the mean square displacement (msd) versus time curves by a linear regression through the first $^1/_3$ of points in individual trajectories (Figure 8A).[116] For the 0.5 and 2 Hz acquisition rate data sets the diffusion coefficients were $(1.8 \pm 0.2) \times 10^{-4}$ and $(4.2 \pm 1.0) \times 10^{-4}$ $\mu m^2/s$, respectively (Table 2). For the 33 Hz acquisition rate data set the diffusion coefficient was $(8.2 \pm 1.5) \times 10^{-3}$ $\mu m^2/s$ (Table 2). However, with this data set the displacements that go into the diffusion coefficient estimation are noise dominated (Table 1). The diffusion coefficients estimated from the 0.5 and 2 Hz data sets are markedly lower than the diffusion coefficients reported for similarly sized or larger *E.coli* plasma membrane proteins[117−119] and therefore suggest that the movement of OmpC is at least partly confined in the outer membrane.[4,112,114] "Confined" diffusion has been frequently observed with membrane proteins and is caused by the interactions of the protein with other membrane components or underlying cytosolic structures.[4,116,120,121] For confined diffusion at a well-defined length scale one would expect to see that the msd curves approach and settle at a plateau. This is not observed for OmpC (Figure 8B). Furthermore, with all data sets we saw little correlation between the duration of a trajectory and the displacement between the initial and final coordinates of the trajectory (Figure 8C). This distance should scale according to $x = (2Dt)^{1/2}$ in "free" Brownian diffusion. If the confinement is not absolute, the protein will occasionally escape the confinement zone and move according to a "normal" Brownian diffusion until being captured by another confinement zone.[114] This may give the appearance of "normal" diffusion in the msd plots when averaged over several escape events. When looking at individual long trajectories (50−70 steps) acquired at 0.5 or 2 Hz we note that they typically dwell in small regions corresponding to the localization error before moving to a nearby neighboring region (Figure 8D and Figure S38B). Several such confinement and escape events may be the reason for the apparent normal diffusion indicated by straight lines in the MSD plot. In Figure 8D we see that the trajectories acquired at 0.5 or 2 Hz approximately reach the normal diffusion distance $(2Dt)^{1/2}$ for 50 to 70 steps as indicated by dashed circles, when the diffusion constant is calculated from the slope of the regression line in the msd plot. Interestingly, the trajectories with durations exceeding 50 steps were located closer to the cell periphery than trajectories consisting of less than 50 steps (Figure S38C,D). For the faster tracking at 33 Hz the trajectories are so short in actual time that they do not leave

DOI: 10.1021/acssynbio.6b00138
ACS Synth. Biol. XXXX, XXX, XXX−XXX

the individual trapping region, and the overall displacement matches the localization error (Figure 8D). Overall the above observations demonstrate that the diffusion of OmpC in the *E.coli* outer membrane is severely restricted. A similarly restricted diffusion has previously been observed in the lateral movement of the *E.coli* outer-membrane maltoporin LamB[122,123] similar to OmpC in size and oligomerization state. As the biological explanation for the restricted movement of OmpC we invoke earlier observations of a direct association of OmpC with the peptidoglycan layer.[124,125] This interaction would tether the OmpC to a limited region of the *E.coli* outer membrane.[124,125] On the basis of a comparison of our msd versus time curves for OmpC with those reported for LamB by Gibbs and co-workers,[123] we note that the msd values observed by us exceed the values observed for LamB by the authors by more than an order of magnitude.[123] We surmise that the higher mobility of OmpC compared to an otherwise similar *E.coli* outer-membrane protein may be due to the retarding[111] or cross-linking[110] effect of the large gold particles used for the labeling of LamB by Gibbs et al.[123] Small molecule fluorescence labeling enables the reduction of those effects. We conclude by noting that the apparently restricted diffusion of OmpC as observed by us adds to the growing body of evidence indicating a compartmentalization of membrane proteins in *E.coli* into microdomains.[118,126,127]

CONCLUSIONS

In this study we report on our attempts to use the NcAA-based small fluorophore tagging to label different *E. coli* proteins for single molecule studies in live cells. We find that the NcAA-incoporation at artificially introduced TAG codons works robustly with diverse NcAAs, though codon context has a major impact on the efficiency of the NcAA incorporation. However, the presence of the TAG stop codon specific release factor RF1 led to a substantial protein truncation at the TAG codon even in the presence of the NcAA-tRNA^{Pyl} as previously observed by others.[56,76,128] The protein truncation and the associated fitness loss is reduced in the recoded *E. coli* strain C321.ΔA.exp where RF1 has been deleted, but the absence of RF1 also led to an increased NcAA-independent TAG codon readthrough. Contrary to our expectations, the endogenous amber codons in a nonrecoded strain did not lead to a significantly increased "off-target" dye incorporation compared to the "amber-less" recoded *E. coli* strain. On this basis, we suggest that the NcAA-based labeling can also be performed in strains where only a subset of amber stop codons have been reassigned and RF1 has been deleted.[56,128−130] The increased misincorporation of endogenous amino acids in the absence of RF1 may be relieved by further evolving the tRNA^{Pyl}/PylRS system[131] or by increasing the expression level of tRNA^{Pyl}.[132] Despite the increased misincorporation of endogenous amino acids at the artificial amber codon in C321.ΔA.exp the incoporation of "clickable" NcAAs yields proteins that can be labeled rapidly using tetrazine fluorophores in intact cells. We find that the dye labeling is selective at the protein level, but causes high fluorescence background when membrane permeable fluorophores are used or when it is limited by the poor membrane permeability of the hydrophilic dyes. This limits the usefulness of click chemistry for intracellular fluorescence labeling in *E. coli*. Nevertheless, the labeling method can be successfully applied to cell-surface exposed proteins in live cells as exemplified by our labeling of the *E. coli* osmoporin OmpC. Labeling of OmpC allowed us to study its diffusive behavior using single molecule tracking and estimate its diffusion coefficient. We speculate that the low mobility of OmpC in the outer membrane of *E. coli* is due to its interactions with the underlying peptidoglycan layer. We conclude that to be easily applicable to the labeling of intracellular proteins in *E. coli*, especially proteins present in low copy numbers where the protein-specific fluorescence signal would be difficult to detect over a high background fluorescence caused by nonspecific dye binding, the labeling method would profit from a further engineering of the fluorescent dyes with regard to their membrane permeability and nonspecific binding as well as the "turn-on" fluorescence upon the "click" reaction. Use of "turn-on" fluorescent dyes[61−63] would also allow the study of transiently expressed proteins.

METHODS

Optical Setup. The optical setup was built around an inverted microscope (Eclipse Ti-E, Nikon) equipped with a high-numerical-aperture objective (CFI Apo TIRF 100xoli N.A. 1.45), a CCD camera (IMAGING SOURCE USB3.0 Monochrome Industrial Camera), and an EMCCD camera (Andor iXon Ultra 897). A 638 nm excitation laser (Genesis MX639-1000-STM, COHERENT) and a 514 nm excitation laser (Genesis CX514-2000 STM, COHERENT) were used as excitation light sources. The following dichroic mirror/emission filter combinations were used to filter fluorescence emission: for the 514 nm light excited emission Di02-R514-25 × 36/FF01-534/27-25 (SEMROCK), for the 638 nm light excited emission LF635-B-000/FF01-676/29-25 (SEMROCK). The fluorescence and brightfield images were acquired on the EMCCD camera, and the phase contrast images were acquired on the CCD camera. Illumination for brightfield and phase-contrast was controlled by a shutter and a shutter driver (Vincent Associates). The cameras, the microscope and the shutter were controlled by μManager 1.4.19.

Plasmids and Strains. TAG-containing variants of LacI and OmpC were made by standard site directed mutagenesis using the AccuPrime Pfx DNA Polymerase (Invitrogen). TAG codons were introduced at the positions Y12, Q153, and A312 in LacI and at the position D311 in OmpC (see Supplementary Table SX for the primer sequences). The positions for TAG insertion were selected based on the existing mutagenesis data[65,66] and an analysis of the following crystal structures: PDB IDs: 1EFA[133] for LacI and 2J1N[68] for OmpC. The TAG-containing PCR fragments were subcloned into pBAD24 between the *Eco*RI and Hind III restriction sites in the case of LacI variants Q153TAG and A312TAG and between the *Bam*HI and *Hin*dIII sites in the case of LacI variant Y12TAG and the OmpC variant D311TAG. The primer sequences used for making the constructs are given in Table S2. The identity of the constructs was verified by sequencing (Table S3). The derivative of pEVOL ("pEVOL-ΔPylRS") lacking both copies of PylRS was made by PCR-amplifying the original pEVOL using primers complementary to the sites flanking the region harboring the PylRS genes and a Phusion Hot-Start DNA polymerase, followed by ligation of the PCR product using T4 DNA ligase. The pBAD24-GFP-Y39TAG construct was from ref 34.

The recoded *E. coli* strain C321.ΔA.exp was obtained from Addgene. The pEVOL containing BW25993 and C321.ΔA.exp strains were obtained by a transformation with the pEVOL plasmid, followed by incubation at 37 °C in LB in the presence of 50 μg/mL chloramphenicol. The pEVOL containing strains

DOI: 10.1021/acssynbio.6b00138
ACS Synth. Biol. XXXX, XXX, XXX−XXX

were subsequently transformed with the pBAD24 expression constructs and incubated at 37 °C in LB in the presence of 50 μg/mL chloramphenicol and 100 μg/mL carbenicillin.

Chemicals. Trans cyclooct-2-ene lysine (TCO*-AK) and endobicyclo[6.1.0]noncyne lysine (BCNK) were obtained from Sirius Fine Chemicals. eBoc lysine (eBocK) was obtained from Iris Biotech GmbH. TAMRA-tetrazine was purchased from Click Chemistry Tools (Scottsdale, Arizona). ATTO532-tetrazine, ATTO647N-tetrazine, sulfo-Cy5-tetrazine, and m6-sulfo-Cy5-tetrazine were purchased from Jena Biosciences. D-biotin, RPMI amino acids (without L-glutamine), and thiamine hydrochloride were from Sigma-Aldrich.

Western Blot Analysis. LacI was transferred from acrylamide gels to Amersham ProtRan Premium 0.45 μm blotting membranes (GE Healthcare Life Sciences) in a TE77 PWR transfer unit (GE Healthcare Life Sciences) at 1 mA/cm^2 at ambient temperature for 40 min. The membranes were rinsed with 15 mL of PBS + 0.1% Tween-20 and blocked with 2.5% milk in PBS + 0.1% Tween-20 at ambient temperature for 2 h. For anti-LacI blotting, the membrane was incubated with mouse monoclonal anti-LacI antibody (IgG_1, clone 9A5, Millipore) in 10 mL of 2.5% milk in PBS + 0.1% Tween-20 at a 1:5000 antibody dilution at ambient temperature for 2 h. The membrane was washed three times with 15 mL of 2.5% milk in PBS + 0.1% Tween-20 at ambient temperature over 30 min. The membrane was subsequently incubated with antimouse horseradish peroxidase conjugate (Jackson Immunoresearch) in 10 mL of PBS + 0.1% Tween-20 at a 1:5000 antibody dilution at ambient temperature for 1 h, followed by three washes with 15 mL of PBS + 0.1% Tween-20 (ambient temperature). The blots were developed using ECL Prime Western Blotting Detection Reagent (Amersham) and visualized on a ChemiDoc MP Imaging System (BioRad).

NcAA Incorporation Analysis into LacI. The efficiency of NcAA incoporation into LacI was analyzed in the recoded *E. coli* strain C321.ΔA.exp harboring the $tRNA^{Pyl}$/PylRS expression plasmid pEVOL (p15 origin of replication, chloramphenicol acetyltransferase for chloramphenicol resistance) and a pBAD24 construct containing the LacI-Y12TAG variant. Cells were grown overnight at 37 °C/200 rpm in Luria−Bertani (LB) medium in the presence of 50 μg/mL chloramphenicol and 100 μg/mL carbenicillin. The overnight cultures were diluted to ΔOD600 = 0.08 in 5 mL of LB containing 50 μg/mL chloramphenicol and 100 μg/mL carbenicillin and supplemented with 0.2% (v/v) L-arabiniose and one of the following NcAAs at a 1 mM final concentration: eBocK, BCNK, or TCO*-AK. A culture expressing LacI from the WT construct was used as a positive control. The cultures were incubated at 37 °C/200 rpm and cells were harvested at ΔOD600 = 2.4−2.8. The cells were pelleted at 12 000*g* at ambient temperature for 1 min and resuspended in 20 μL 1× Laemmli Sample Buffer (BioRad) (+ 0.35 M β-mercaptoethanol). The samples were incubated at 95 °C for 10 min and centrifuged at 12 000*g* for 1 min; 15 μL of supernatants was run in a 4%−15% acrylamide gel (BioRad). LacI levels in the gels were analyzed by Western blot as described above.

The incorporation efficiencies of TCO*-AK into LacI in dependence of the location of the TAG codon in the LacI gene were analyzed in the recoded strain C321.ΔA.exp and in the nonrecoded strain BW25993 genotypically similar to the MG1655-derived EcN2 parent strain used for the construction of the strain C321.ΔA.exp.[56] The cells were grown in the presence of 50 μg/mL chloramphenicol and 100 μg/mL carbenicillin in 2 mL of LB medium supplemented with 0.02% (v/v) L-arabinose and 1 mM TCO*-AK at 37 °C/200 rpm. At culture densities ΔOD600 = 0.8−1.0 (time point 1) and ΔOD600 = 3−6 (time point 2) aliquots with a volume of 750 μL/1 ΔOD600 unit were withdrawn from the cultures and cells pelleted at 12 000*g* at ambient temperature for 1 min. The pellets were washed four times 40 min with 500 μL of PBS at 37 °C/200 rpm. Between washes cells were pelleted at 1700*g* at ambient temperature for 4 min and resuspended by pipetting. After being washed, the cells were resuspended in 30−80 μL of "Lysis Buffer" ["BugBuster" Lysis reagent (Novagen), 0.1 ug/mL egg white lyzozyme (AppliChem), 0.05 U/μL Dnase I (Invitrogen)] to yield suspensions with a nominal density of ΔOD600 = 3. The lysates were incubated at ambient temperature for 40 min, followed by clearing with the use of centrifugation at 12 000*g* for 1 min. A 25 μL aliquot of supernatants was mixed with ATTO647N-tet to a final concentration of 1 μM and incubated at 37 °C/200 rpm for 30 min. The samples were run in 12% precast acrylamide gels (BioRad) and analyzed for dye fluorescence on a ChemiDoc Imaging System. LacI levels in the gels were analyzed by Western blot as described above.

In-gel Fluorescence Analysis of LacI and OmpC Labeling. Cells harboring the LacI-TAG or OmpC-TAG pBAD24 constructs were grown overnight in LB at 37 °C/200 rpm in the presence of 50 μg/mL chloramphenicol and 100 μg/mL carbenicillin. The cells were diluted to a ΔOD600 = 0.08 in 8 mL LB containing 50 μg/mL chloramphenicol and 100 μg/mL carbenicillin and supplemented with 1 mM TCO*-AK and 0.2% (v/v) L-arabiniose. The cultures were incubated at 30 °C for OmpC expression and 37 °C for LacI expression at 200 rpm. The cells were harvested for labeling at the following densities: for LacI, ΔOD600 = 1.8; for OmpC = 0.8. The cells were pelleted in at 5000*g*/*RT* for 5 min, quickly rinsed with 1 mL PBS and then washed with 1 mL PBS in 5 successive washing steps at 37 °C/200 rpm for 10 min. The cells were pelleted at 1700*g* for 4 min at ambient temperature and initially resuspended in 300 μL PBS. The densities of the suspensions were subsequently adjusted to ΔOD600 = 9 with PBS. Two pairs of 150 μL aliquots were withdrawn from each of the ΔOD600 = 9 suspensions. In one of the pair of aliquots the cells were pelleted at 12 000*g* at ambient temperature for 30 s and resuspended in 150 μL "Lysis buffer" ["BugBuster" Lysis reagent, 0.1 ug/mL egg white lyzozyme (AppliChem), 0.05 U/μL Dnase I (Invitrogen)]. The lysates were incubated at ambient temperature for 40 min. The lysates were cleared by centrifugation at 12 000*g* at ambient temperature for 1 min and the ca. 140 μL of supernatants transferred to new tubes. In the other of the pair of aliquots the cells were incubated at ambient temperature for 40 min alongside with the lysates. From the cell suspensions and the lysate supernatants 20 μL aliquots were withdrawn to new tubes and mixed with the following tetrazine dyes (to a final concentration of the dye 5 μM): TAMRA-tet, ATTO647N-tet, Cy5-tet, sulfo-Cy5-tet, m6-sulfo-Cy5-tet. The samples were incubated at 37°/200 rpm for 40 min wrapped in an aluminum foil. Ten microliter aliquots of the labeling samples were withdrawn, incubated at 95 °C/10 min and cleared by centrifugation at 12 000*g* at ambient temperature for 1 min. The cleared supernatants were run in 12% Mini-PROTEAN TGX precast acrylamide gels (BioRad) and visualized for dye fluorescence on a ChemiDoc Imaging System. Fluorescent gels were analyzed in ImageJ image processing software.

DOI: 10.1021/acssynbio.6b00138
ACS Synth. Biol. XXXX, XXX, XXX−XXX

LacI Tetramerization Analysis. All LacI variants were expressed from pBAD24 in 15 mL of LB at 37 °C in the presence of 0.02% (v/v) L-arabinose for 6 h. The N-terminally His6-tagged LacI variants LacI-Y12TCO*-AK, LacI-A312TCO*-AK, and LacI-WT were expressed in *E. coli* C321.ΔA.exp/pEVOL. The C-terminally His6-tagged LacI-WT ("LacI-Dim") was expressed in *E. coli* BW25993. In "LacI-Dim" the His6 purification tag replaces the C-terminal tetramerization helix, abolishing the tetramerization of the protein. The LacI- Y12TCO*-AK and LacI-A312TCO*-AK variants were expressed in the presence of 1 mM TCO*-AK. Cells were pelleted at 7200*g*/ambient temperature for 6 min, and the pellets were washed with 1 mL of PBS in five centrifugation (12 000*g*/ambient temperature for 1 min) and resuspension steps. Between the centrifugations, suspensions were incubated at 37 °C/200 rpm for 40 min.

The cells were lyzed by resuspending them in 400 μL of "BugBuster" protein extraction reagent (Novagen) (75 μg/mL lyzozyme [AppliChem], 0.2 U Dnase I [Invitrogen]) and incubating the lysates at ambient temperature for 30 min. The lysates were centrifuged at 12 000*g*/ambient temperature for 10 min. The lysate supernatants (ca. 400 μL) were mixed with a 500 μL Ni-NTA (QIAGen) suspension in buffer A (20 mM KH_2PO_4/K_2HPO_4 (pH 7.4), 500 mM NaCl, 20 mM Imidazole) and incubated at 4 °C on a rotary shaker for 1 h. The Ni-NTA gel was spun down at 1680*g*/ambient temperature for 30 s, followed by removal of the supernatant. The Ni-NTA gel was resuspended in 300 μL of buffer A and the suspensions were transferred to "Mini BioSpin" columns. The Ni-NTA gel was washed seven times with 300 μL buffer A at ambient temperature to remove unbound protein. Ni-NTA bound LacI was eluted from the gel in 150 μL buffer B (20 mM KH_2PO_4/K_2HPO_4 (pH 7.4), 500 mM NaCl, 500 mM Imidazole) at ambient temperature. The eluates were clarified by centrifugation at 12 000*g*/ambient temperature for 1 min. The supernatants were mixed with sulfo-Cy5-tet to a final concentration of 5 μM and incubated at 37 °C/200 rpm for 30 min. The labeling mixtures were transferred to Amicon Ultra 3-K 3 kDa Mw cutoff centrifugal filters and centrifuged at 13 000*g*/4 °C until 50 μL retentate was left on the filters. The retentates were washed two times with 450 μL "LacI buffer" (25 mM Tris-HCl (pH 7.9), 5 mM $MgCl_2$, 100 mM KCl) and concentrated to a volume of 30 μL. A 1−6 μL aliquot of the sample in 1× loading buffer (31.3 mM Tris-HCl (pH 6.8), 12% glycerol) was loaded onto a 12% acrylamide gel (BioRad) and run in native PAGE running buffer (25 mM Tris-HCl (pH 8.3), 192 mM glycine) at 100 V/8 mA/4 °C for 7 h. In-gel fluorescence and Western blot analysis of the gel was performed as described above.

To verify the charge of the LacI variants at pH 8.3 of the native PAGE gel, isolectric points (pI) for the LacI variants were calculated based on the amino acid sequences using the ExPASy web server (http://web.expasy.org/compute_pi/). To calculate the pI for the sulfo-Cy5-tet labeled LacI-Y12TCO*-AK and LacI-A312TCO*-AK variants, we first calculated the pI of the TCO*-AK-sulfo-Cy5-tet conjugate using "Marvin Sketch" version 16.6.27 software (Chemaxon). The pIs of the entire TCO*-AK-sulfo-Cy5-tet bearing LacI variants were then calculated from the amino acid sequences of LacI by replacing the amino acid at the NcAA incorporation position with cysteine. Cysteine was selected for the replacement due to the closeness of its pI (5.02) to the pI of the TCO*-AK-sulfo-Cy5-tet conjugate (pI = 4.89).

Fluorescence Labeling of LacI for Microscopy. For LacI labeling, cells were grown in LB at 37 °C as described in the "In-gel fluorescence analysis of LacI and OmpC labeling" section and harvested for labeling at the following densities: ΔOD600 = 0.6 (exponential phase) and ΔOD600 = 2−3 (stationary phase). The cells were collected by centrifugation at 5000*g* at ambient temperature for 5 min. The pellets were washed with 1 mL of LB in seven to eight successive 1 h washing steps at 37 °C/200 rpm. Between washes cells were collected by centrifugation at 1700*g* at ambient temperature for 4 min. The cells were then resuspended in 1 mL of PBS and left overnight on a shaker at ambient temperature. Prior to labeling, the densities of the cell suspensions were adjusted to ΔOD600 = 3 with PBS. The ΔOD600 = 3 suspensions were mixed with the tetrazine fluorophore to a final concentration of 0.1 or 2 μM and incubated at 37 °C/200 rpm for 30 min. The cells were collected by centrifugation at 1700*g* at ambient temperature for 4 min. The pellets were washed with 1 mL of LB in seven to eight successive 1 h washing steps at 37 °C/200 rpm. Between washes cells were collected by centrifugation at 1700*g* at ambient temperature for 4 min. The cells were then resuspended in 1 mL of PBS and left overnight on a shaker at ambient temperature. In the dye electroporation experiments cells were subsequently washed with 6 × 1 mL of ice-cold 10% (v/v) glycerol and resuspended in 10% ice-cold glycerol to a ΔOD600 = 16. Then, 50 μL samples of the glycerol-washed suspensions were mixed with sulfo-Cy5-tet to a final concentration of 2 μM and electroporated in presterilized 0.1 cm gap-width electroporation cuvettes (Molecular Bioproducts, Inc.) at a field density of 1.8 kV/cm in a MicroPulser electroporation apparatus (BioRad). Immediately upon electroporation the samples were diluted with 200 μL of LB, and cells were recovered at 37 °C for 1.5 h followed by 6 washes with 1 mL of LB over 12 h on a shaker at ambient temperature.

Fluorescence Labeling of OmpC for Microscopy. C321.ΔA.exp or BW25993 cells harboring pEVOL and the pBAD24-OmpC-D311TAG or pBAD24-OmpC-WT constructs were grown overnight in LB at 37 °C/200 rpm in the presence of 50 μg/mL chloramphenicol and 100 μg/mL carbenicillin. The cells were diluted to a ΔOD600 = 0.08 in M9/0.7% glycerol/1×RPMI amino acids/15% LB and grown at 26 °C/200 rpm in the presence of 1 mM TCO*-AK and 0.02% L-arabinose (for OmpC-D311TCO*-AK) or 0.0002% L-arabinose (for OmpC-WT). At ΔOD600 = 0.5−0.9 cells were collected by centrifugation at 7200*g* ambient temperature for 15 min and washed 5 times with the growth medium at 37 °C/200 rpm over 5 h. Between washes, cells were collected by centrifugation at 1700*g* at ambient temperature for 4 min. The cells were resuspended in 1 mL of M9/0.8% glycerol and left on a rotary shaker at 4 °C overnight. Cells were then resuspended in PBS to ΔOD600 = 3 and incubated with 10 nM tetrazine fluorophores at 37 °C for 20 min. Subsequently, cells were first washed with 1 mL of M9/0.7% glycerol/1×RPMI amino acids/15% LB at 37 °C/200 rpm over 1 h and then 5 times with 1 mL of M9/0.8% glycerol at 37 °C/200 rpm over 5 h.

Fluorescence Imaging of Dye Treated Cells on Agarose Pads. After the dye washout the densities of the cell suspensions were adjusted to ΔOD600 = 30, and 0.6 μL samples from those suspensions were pipetted on 4 × 4 mm 2% agarose pads (in M9 plus 0.8% glycerol). The pads were air-dried at ambient temperature for 5 min and sealed with a Hellmanex-III (Sigma) cleaned coverslip. The imaging specimen was mounted on a Nikon Ti Inverted microscope with the

DOI: 10.1021/acssynbio.6b00138
ACS Synth. Biol. XXXX, XXX, XXX−XXX

cell-covered side facing the objective. If not stated otherwise, the fluorescence images were aquired at beam intensities of 10 W/cm^2 (for Cy5-tet and ATTO647N-tet in LacI labeling) or 60 W/cm^2 (for sulfo-Cy5-tet in OmpC labeling) of the 638 nm laser at the sample plane. Cells receiving no dye treatment were imaged as controls for background subtraction. White light images were aquired using a white light lamp (Nikon Instruments) and a condenser (TI-DF, Nikon Instruments) attached to the microscope as an illumination source.

Fluorescence images were processed using Matlab and visualized with ImageJ. Owing to a considerable cell-to-cell variability in fluorescence uptake, the fluorescence images were processed with a view of obtaining a balanced display of both the highly and dimly fluorescent cells. The contrast-brightness of the images was adjusted to a common intensity scale in the following way (Figure S39). The lower pixel intensity threshold was set equal to the mean plus three standard deviations of the intensity of the images of cells receiving no dye treatment. The upper pixel intensity threshold for the contrast adjustment was calculated in two steps. First, pixel intensities from all images in a sample were concatenated into a single intensity matrix and the mean and standard deviation were calculated based on the first and second quartile of the collected pixel intensities. The upper threshold for the contrast adjustment was then set equal to the mean plus three standard deviations of the sample with the highest mean fluorescence signal.

Sample Preparation and Setup for OmpC Imaging in Microfluidic Chips. The design, fabrication, and preparation of microfluidic chips have been described previously.[134] Briefly, port holes (0.5 mm diameter) were punched out of the chip. The chip was cleaned using scotch tape, and the chip and a coverslip (40 mm diameter, 200 μm thick, Thermo-Scientific) were then further cleaned by oxygen/UV plasma treatment (UVO-cleaner 42-220, Jellight Co.) for 10 min followed by treatment of both surfaces to be bonded with a high frequency generator (ETP MODEL BD-20 V, Electro-Technic Products, Inc.). The chip was dropped onto the treated surface of the coverslip, and the bond was stabilized at 80 °C for 10 min. Just prior to loading and running the chip, it was flooded with deionized water.

Cells harboring the OmpC-D311TAG construct were grown overnight at 37 °C/200 rpm in the presence of 50 μg/mL chloramphenicol and 100 μg/mL carbenicillin. The cells were diluted to ΔOD600 = 0.08 in 100 mL of M9 containing 0.7% glycerol and supplemented with 1 mM TCO*-AK, 0.15% (v/v) L-arabinose and 15% (v/v) LB. Cells were grown at 26 °C/200 rpm and harvested at ΔOD600 = 0.311. The cells were spun at 10 000g/ambient temperature for 10 min and washed 6 times with 2 mL of growth medium over 5 h at ambient temperature. Between washes cells were collected by centrifugation at 1700g at ambient temperature for 4 min. The cells were kept at 4 °C overnight in M9 plus 0.7% glycerol. On the following day the cells were additionally washed 3 times with M9 plus 0.7% glycerol at ambient temperature over 1.5 h and resuspended in M9 plus 0.8% glycerol to a density ΔOD600 = 3.7. The cell suspension was mixed with sulfo-Cy5-tet to a final concentration of 10 nM and incubated at 37 °C/200 rpm for 20 min. The cells were then pelleted at 1700g at ambient temperature and washed 7 times with 1 mL M9 plus 0.8% glycerol at ambient temperature over 4 h. The suspensions were stored at 4 °C overnight. On the following day the cells were pelleted at 1700g at ambient temperature and resuspended in 600 μL of M9 plus 0.4% glycerol.

In preparation for the cell loading, reservoirs connected to the microfluidic chip were filled with sterile "chip growth" medium (M9, 0.4% glucose, 1×RPMI amino acids, 0.02% (v/v) pluronic, 0.15 μg/mL D-biotin, 1 μg/mL thiamine hydrochloride), and the medium was degassed for approximately 40 min. The flow inside the microfluidic chip was controlled by adjusting the elevation of the media reservoirs relative to the sample. A 50 μL aliquot of the cells harboring Cy5-labeled OmpC was spun down at 12000g for 30 s, concentrated in 200 μL of fresh "chip growth" medium and introduced into the chip through the running waste port. Cells were caught in the traps by introducing pressure waves into the tubing by manually shaking the tubing, and once all traps were sufficiently occupied (approximately 5−50 cells per trap), the direction of the flow in the chamber was reversed, such that cells outside the traps were exchanged with fresh medium. The cells were allowed to acclimatize and grow at 37 °C for approximately 7 h before imaging. The temperature was maintained using a custom-fitted incubator hood (OKO LAB).

Each microcolony in a trap was imaged at a frame rate of 0.5 or 2 Hz for a total of 200 frames (100 or 400 s) with an excitation laser exposure time of 150 ms (for the 2 Hz set) or 250 ms (for the 0.5 Hz set) per single frame at a beam intensity of 290−660 W/cm^2 of the 638 nm laser at the sample plane. The fluorescence movies and brightfield images were acquired on the EMCCD camera. The phase-contrast images were acquired on the CCD chamera. The EMCCD camera gain was set to 300 during the image acquisition.

Cell Geometry Determination and Analysis of Fluorescence Images of Cells in Microfluidic Devices. Cell contours of the cells imaged in the microfluidic devices were determined from phase-contrast images. The phase contrast images were first brought into register with the brightfield images to allow the fluorescence movies to be overlaid on the segmented images. A cell segmentation algorithm was then used to detect cells in phase contrast images.[135] Cell width and length were computed using the segmented cells to create an internal coordinate system.

An à trous wavelet three-plane decomposition was used for spot detection.[136] The spots were detected in the second wavelet plane and significant wavelet coefficients were determined through scale-dependent kσ-thresholding where σ is the standard deviation of the second wavelet plane. The standard deviation was estimated by the median absolute deviation method[137] and k was set to 3.5. The spot centers were determined by a weighted centroid calculation from the pixel regions obtained from the wavelet analysis. The frame coordinates of each fluorescent particle were mapped into a coordinate system internal to a segmented cell and the trajectories of the fluorescent particles were constructed by connecting points from consecutive frames in the fluorescent movies and were kept if they consisted of at least 10 points. The maximum allowed xy frame-to-frame displacements were set to 250 nm. The diffusion coefficient and particle localization errors were estimated from the mean-squared displacement (msd) versus time curves of individual trajectories by a linear regression. Points up to $^1/_3$ of the maximal time lag for each trajectory were used for the regression.

■ ASSOCIATED CONTENT

Supporting Information

The Supporting Information is available free of charge on the ACS Publications website at DOI: 10.1021/acssynbio.6b00138.

DOI: 10.1021/acssynbio.6b00138
ACS Synth. Biol. XXXX, XXX, XXX−XXX

Table S1 with the sequences of *M.mazei* $tRNA^{Pyl}$ and $PylRS^{AF}$; Table S2 with primer sequences used in the study, supplementary methods, Figures S1−S36 (incl. NcAA and dye structures, NcAA incorporation sites in LacI and OmpC, controls for the labeling) (PDF)

AUTHOR INFORMATION

Corresponding Author

*E-mail: johan.elf@icm.uu.se.

Notes

The authors declare no competing financial interest.

ACKNOWLEDGMENTS

We thank Drs. Anthony C. Forster and Sanna Koskiniemi for helpful discussions, Alex Boucharin for help with image analysis, and Dr. Cecilia Unoson for providing the PylRS-free pEVOL expression plasmid. We are especially grateful to Irmely Barkefors for a critical reading of the manuscript. This work was supported by the European Research Council, the Swedish Research Council, and the Knut and Alice Walleberg Foundation. I.N. acknowledges financial support by the European Commission Seventh Framework Programme (FP7) through Marie Curie Actions (FP7-PEOPLE-IEF) and a European Molecular Biology Organization (EMBO) long-term fellowship. E.A.L. acknowledges funding from the SPP1623 and the Emmy Noether program of the DFG.

REFERENCES

(1) Giepmans, B. N., Adams, S. R., Ellisman, M. H., and Tsien, R. Y. (2006) The fluorescent toolbox for assessing protein location and function. *Science 312*, 217−224.

(2) Gahlmann, A., and Moerner, W. E. (2014) Exploring bacterial cell biology with single-molecule tracking and super-resolution imaging. *Nat. Rev. Microbiol. 12*, 9−22.

(3) Persson, F., Linden, M., Unoson, C., and Elf, J. (2013) Extracting intracellular diffusive states and transition rates from single-molecule tracking data. *Nat. Methods 10*, 265−269.

(4) Clausen, M. P., and Lagerholm, B. C. (2011) The probe rules in single particle tracking. *Curr. Protein Pept. Sci. 12*, 699−713.

(5) Ha, T., and Tinnefeld, P. (2012) Photophysics of fluorescent probes for single-molecule biophysics and super-resolution imaging. *Annu. Rev. Phys. Chem. 63*, 595−617.

(6) Landgraf, D., Okumus, B., Chien, P., Baker, T. A., and Paulsson, J. (2012) Segregation of molecules at cell division reveals native protein localization. *Nat. Methods 9*, 480−482.

(7) Wang, S., Moffitt, J. R., Dempsey, G. T., Xie, X. S., and Zhuang, X. (2014) Characterization and development of photoactivatable fluorescent proteins for single-molecule-based superresolution imaging. *Proc. Natl. Acad. Sci. U. S. A. 111*, 8452−8457.

(8) Ghodke, H., Caldas, V. E., Punter, C. M., van Oijen, A. M., and Robinson, A. (2016) Single-Molecule Specific Mislocalization of Red Fluorescent Proteins in Live Escherichia coli. *Biophys. J. 111*, 25−27.

(9) Keppler, A., Gendreizig, S., Gronemeyer, T., Pick, H., Vogel, H., and Johnsson, K. (2003) A general method for the covalent labeling of fusion proteins with small molecules in vivo. *Nat. Biotechnol. 21*, 86−89.

(10) Gautier, A., Juillerat, A., Heinis, C., Correa, I. R., Jr., Kindermann, M., Beaufils, F., and Johnsson, K. (2008) An engineered protein tag for multiprotein labeling in living cells. *Chem. Biol. 15*, 128−136.

(11) Los, G. V., Encell, L. P., McDougall, M. G., Hartzell, D. D., Karassina, N., Zimprich, C., Wood, M. G., Learish, R., Ohana, R. F., Urh, M., Simpson, D., Mendez, J., Zimmerman, K., Otto, P., Vidugiris, G., Zhu, J., Darzins, A., Klaubert, D. H., Bulleit, R. F., and Wood, K. V. (2008) HaloTag: a novel protein labeling technology for cell imaging and protein analysis. *ACS Chem. Biol. 3*, 373−382.

(12) Miller, L. W., and Cornish, V. W. (2005) Selective chemical labeling of proteins in living cells. *Curr. Opin. Chem. Biol. 9*, 56−61.

(13) Wombacher, R., Heidbreder, M., van de Linde, S., Sheetz, M. P., Heilemann, M., Cornish, V. W., and Sauer, M. (2010) Live-cell super-resolution imaging with trimethoprim conjugates. *Nat. Methods 7*, 717−719.

(14) Popp, M. W., Antos, J. M., Grotenbreg, G. M., Spooner, E., and Ploegh, H. L. (2007) Sortagging: a versatile method for protein labeling. *Nat. Chem. Biol. 3*, 707−708.

(15) Chen, I., Howarth, M., Lin, W. Y., and Ting, A. Y. (2005) Site-specific labeling of cell surface proteins with biophysical probes using biotin ligase. *Nat. Methods 2*, 99−104.

(16) Howarth, M., and Ting, A. Y. (2008) Imaging proteins in live mammalian cells with biotin ligase and monovalent streptavidin. *Nat. Protoc. 3*, 534−545.

(17) Uttamapinant, C., White, K. A., Baruah, H., Thompson, S., Fernandez-Suarez, M., Puthenveetil, S., and Ting, A. Y. (2010) A fluorophore ligase for site-specific protein labeling inside living cells. *Proc. Natl. Acad. Sci. U. S. A. 107*, 10914−10919.

(18) Cohen, J. D., Zou, P., and Ting, A. Y. (2012) Site-Specific Protein Modification Using Lipoic Acid Ligase and Bis-Aryl Hydrazone Formation. *ChemBioChem 13*, 888−894.

(19) Liu, D. S., Nivon, L. G., Richter, F., Goldman, P. J., Deerinck, T. J., Yao, J. Z., Richardson, D., Phipps, W. S., Ye, A. Z., Ellisman, M. H., Drennan, C. L., Baker, D., and Ting, A. Y. (2014) Computational design of a red fluorophore ligase for site-specific protein labeling in living cells. *Proc. Natl. Acad. Sci. U. S. A. 111*, E4551−E4559.

(20) Griffin, B. A., Adams, S. R., and Tsien, R. Y. (1998) Specific covalent labeling of recombinant protein molecules inside live cells. *Science 281*, 269−272.

(21) Adams, S. R., Campbell, R. E., Gross, L. A., Martin, B. R., Walkup, G. K., Yao, Y., Llopis, J., and Tsien, R. Y. (2002) New biarsenical ligands and tetracysteine motifs for protein labeling in vitro and in vivo: synthesis and biological applications. *J. Am. Chem. Soc. 124*, 6063−6076.

(22) Gaietta, G., Deerinck, T. J., Adams, S. R., Bouwer, J., Tour, O., Laird, D. W., Sosinsky, G. E., Tsien, R. Y., and Ellisman, M. H. (2002) Multicolor and electron microscopic imaging of connexin trafficking. *Science 296*, 503−507.

(23) Wurm, C. A., Suppanz, I. E., Stoldt, S., and Jakobs, S. (2010) Rapid FlAsH labelling in the budding yeast Saccharomyces cerevisiae. *J. Microsc. 240*, 6−13.

(24) Fessenden, J. D., and Mahalingam, M. (2013) Site-Specific Labeling of the Type 1 Ryanodine Receptor Using Biarsenical Fluorophores Targeted to Engineered Tetracysteine Motifs. *PLoS One 8*, e64686.

(25) Stroffekova, K., Proenza, C., and Beam, K. G. (2001) The protein-labeling reagent FLASH-EDT2 binds not only to CCXXCC motifs but also non-specifically to endogenous cysteine-rich proteins. *Pfluegers Arch. 442*, 859−866.

(26) Stohr, K., Siegberg, D., Ehrhard, T., Lymperopoulos, K., Oz, S., Schulmeister, S., Pfeifer, A. C., Bachmann, J., Klingmuller, U., Sourjik, V., and Herten, D. P. (2010) Quenched substrates for live-cell labeling of SNAP-tagged fusion proteins with improved fluorescent background. *Anal. Chem. 82*, 8186−8193.

(27) Bosch, P. J., Correa, I. R., Jr., Sonntag, M. H., Ibach, J., Brunsveld, L., Kanger, J. S., and Subramaniam, V. (2014) Evaluation of fluorophores to label SNAP-tag fused proteins for multicolor single-molecule tracking microscopy in live cells. *Biophys. J. 107*, 803−814.

(28) Fernandez-Suarez, M., Baruah, H., Martinez-Hernandez, L., Xie, K. T., Baskin, J. M., Bertozzi, C. R., and Ting, A. Y. (2007) Redirecting lipoic acid ligase for cell surface protein labeling with small-molecule probes. *Nat. Biotechnol. 25*, 1483−1487.

(29) Slavoff, S. A., Chen, I., Choi, Y. A., and Ting, A. A. Y. (2008) Expanding the substrate tolerance of biotin ligase through exploration of enzymes from diverse species. *J. Am. Chem. Soc. 130*, 1160−1162.

DOI: 10.1021/acssynbio.6b00138
ACS Synth. Biol. XXXX, XXX, XXX−XXX

(30) Wang, J., Xie, J., and Schultz, P. G. (2006) A genetically encoded fluorescent amino acid. *J. Am. Chem. Soc. 128*, 8738−8739.
(31) Summerer, D., Chen, S., Wu, N., Deiters, A., Chin, J. W., and Schultz, P. G. (2006) A genetically encoded fluorescent amino acid. *Proc. Natl. Acad. Sci. U. S. A. 103*, 9785−9789.
(32) Charbon, G., Brustad, E., Scott, K. A., Wang, J., Lobner-Olesen, A., Schultz, P. G., Jacobs-Wagner, C., and Chapman, E. (2011) Subcellular protein localization by using a genetically encoded fluorescent amino acid. *ChemBioChem 12*, 1818−1821.
(33) Mittelstaet, J., Konevega, A. L., and Rodnina, M. V. (2013) A kinetic safety gate controlling the delivery of unnatural amino acids to the ribosome. *J. Am. Chem. Soc. 135*, 17031−17038.
(34) Plass, T., Milles, S., Koehler, C., Schultz, C., and Lemke, E. A. (2011) Genetically encoded copper-free click chemistry. *Angew. Chem., Int. Ed. 50*, 3878−3881.
(35) Lang, K., Davis, L., Wallace, S., Mahesh, M., Cox, D. J., Blackman, M. L., Fox, J. M., and Chin, J. W. (2012) Genetic Encoding of bicyclononynes and trans-cyclooctenes for site-specific protein labeling in vitro and in live mammalian cells via rapid fluorogenic Diels-Alder reactions. *J. Am. Chem. Soc. 134*, 10317−10320.
(36) Lang, K., Davis, L., Torres-Kolbus, J., Chou, C., Deiters, A., and Chin, J. W. (2012) Genetically encoded norbornene directs site-specific cellular protein labelling via a rapid bioorthogonal reaction. *Nat. Chem. 4*, 298−304.
(37) Nikic, I., Plass, T., Schraidt, O., Szymanski, J., Briggs, J. A., Schultz, C., and Lemke, E. A. (2014) Minimal tags for rapid dual-color live-cell labeling and super-resolution microscopy. *Angew. Chem., Int. Ed. 53*, 2245−2249.
(38) Nikic, I., Kang, J. H., Girona, G. E., Aramburu, I. V., and Lemke, E. A. (2015) Labeling proteins on live mammalian cells using click chemistry. *Nat. Protoc. 10*, 780−791.
(39) Agard, N. J., Prescher, J. A., and Bertozzi, C. R. (2004) A strain-promoted [3 + 2] azide-alkyne cycloaddition for covalent modification of biomolecules in living systems. *J. Am. Chem. Soc. 126*, 15046−15047.
(40) Baskin, J. M., Prescher, J. A., Laughlin, S. T., Agard, N. J., Chang, P. V., Miller, I. A., Lo, A., Codelli, J. A., and Bertozzi, C. R. (2007) Copper-free click chemistry for dynamic in vivo imaging. *Proc. Natl. Acad. Sci. U. S. A. 104*, 16793−16797.
(41) Blackman, M. L., Royzen, M., and Fox, J. M. (2008) Tetrazine ligation: fast bioconjugation based on inverse-electron-demand Diels-Alder reactivity. *J. Am. Chem. Soc. 130*, 13518−13519.
(42) Karver, M. R., Weissleder, R., and Hilderbrand, S. A. (2011) Synthesis and evaluation of a series of 1,2,4,5-tetrazines for bioorthogonal conjugation. *Bioconjugate Chem. 22*, 2263−2270.
(43) Selvaraj, R., and Fox, J. M. (2013) trans-Cyclooctene–a stable, voracious dienophile for bioorthogonal labeling. *Curr. Opin. Chem. Biol. 17*, 753−760.
(44) Patterson, D. M., Nazarova, L. A., and Prescher, J. A. (2014) Finding the right (bioorthogonal) chemistry. *ACS Chem. Biol. 9*, 592−605.
(45) Wagner, J. A., Mercadante, D., Nikic, I., Lemke, E. A., and Grater, F. (2015) Origin of Orthogonality of Strain-Promoted Click Reactions. *Chem. - Eur. J. 21*, 12431−12435.
(46) Devaraj, N. K., Weissleder, R., and Hilderbrand, S. A. (2008) Tetrazine-based cycloadditions: application to pretargeted live cell imaging. *Bioconjugate Chem. 19*, 2297−2299.
(47) Uttamapinant, C., Howe, J. D., Lang, K., Beranek, V., Davis, L., Mahesh, M., Barry, N. P., and Chin, J. W. (2015) Genetic code expansion enables live-cell and super-resolution imaging of site-specifically labeled cellular proteins. *J. Am. Chem. Soc. 137*, 4602−4605.
(48) Ryu, Y. H., and Schultz, P. G. (2006) Efficient incorporation of unnatural amino acids into proteins in Escherichia coli. *Nat. Methods 3*, 263−265.
(49) Ambrogelly, A., Gundllapalli, S., Herring, S., Polycarpo, C., Frauer, C., and Soll, D. (2007) Pyrrolysine is not hardwired for cotranslational insertion at UAG codons. *Proc. Natl. Acad. Sci. U. S. A. 104*, 3141−3146.
(50) Neumann, H., Peak-Chew, S. Y., and Chin, J. W. (2008) Genetically encoding N(epsilon)-acetyllysine in recombinant proteins. *Nat. Chem. Biol. 4*, 232−234.
(51) Nguyen, D. P., Lusic, H., Neumann, H., Kapadnis, P. B., Deiters, A., and Chin, J. W. (2009) Genetic encoding and labeling of aliphatic azides and alkynes in recombinant proteins via a pyrrolysyl-tRNA Synthetase/tRNA(CUA) pair and click chemistry. *J. Am. Chem. Soc. 131*, 8720−8721.
(52) Nozawa, K., O'Donoghue, P., Gundllapalli, S., Araiso, Y., Ishitani, R., Umehara, T., Soll, D., and Nureki, O. (2009) Pyrrolysyl-tRNA synthetase-tRNA(Pyl) structure reveals the molecular basis of orthogonality. *Nature 457*, 1163−1167.
(53) O'Donoghue, P., Ling, J., Wang, Y. S., and Soll, D. (2013) Upgrading protein synthesis for synthetic biology. *Nat. Chem. Biol. 9*, 594−598.
(54) Chin, J. W. (2014) Expanding and reprogramming the genetic code of cells and animals. *Annu. Rev. Biochem. 83*, 379−408.
(55) Devaraj, N. K., and Weissleder, R. (2011) Biomedical applications of tetrazine cycloadditions. *Acc. Chem. Res. 44*, 816−827.
(56) Lajoie, M. J., Rovner, A. J., Goodman, D. B., Aerni, H. R., Haimovich, A. D., Kuznetsov, G., Mercer, J. A., Wang, H. H., Carr, P. A., Mosberg, J. A., Rohland, N., Schultz, P. G., Jacobson, J. M., Rinehart, J., Church, G. M., and Isaacs, F. J. (2013) Genomically recoded organisms expand biological functions. *Science 342*, 357−360.
(57) Elf, J., Li, G. W., and Xie, X. S. (2007) Probing transcription factor dynamics at the single-molecule level in a living cell. *Science 316*, 1191−1194.
(58) Hammar, P., Leroy, P., Mahmutovic, A., Marklund, E. G., Berg, O. G., and Elf, J. (2012) The lac repressor displays facilitated diffusion in living cells. *Science 336*, 1595−1598.
(59) Hammar, P., Wallden, M., Fange, D., Persson, F., Baltekin, O., Ullman, G., Leroy, P., and Elf, J. (2014) Direct measurement of transcription factor dissociation excludes a simple operator occupancy model for gene regulation. *Nat. Genet. 46*, 405−408.
(60) Winter, R. B., Berg, O. G., and von Hippel, P. H. (1981) Diffusion-driven mechanisms of protein translocation on nucleic acids. 3. The Escherichia coli lac repressor–operator interaction: kinetic measurements and conclusions. *Biochemistry 20*, 6961−6977.
(61) Herner, A., Nikic, I., Kallay, M., Lemke, E. A., and Kele, P. (2013) A new family of bioorthogonally applicable fluorogenic labels. *Org. Biomol. Chem. 11*, 3297−3306.
(62) Herner, A., Estrada Girona, G., Nikic, I., Kallay, M., Lemke, E. A., and Kele, P. (2014) New generation of bioorthogonally applicable fluorogenic dyes with visible excitations and large Stokes shifts. *Bioconjugate Chem. 25*, 1370−1374.
(63) Meimetis, L. G., Carlson, J. C., Giedt, R. J., Kohler, R. H., and Weissleder, R. (2014) Ultrafluorogenic coumarin-tetrazine probes for real-time biological imaging. *Angew. Chem., Int. Ed. 53*, 7531−7534.
(64) Young, T. S., Ahmad, I., Yin, J. A., and Schultz, P. G. (2010) An enhanced system for unnatural amino acid mutagenesis in E. coli. *J. Mol. Biol. 395*, 361−374.
(65) Kleina, L. G., and Miller, J. H. (1990) Genetic studies of the lac repressor. XIII. Extensive amino acid replacements generated by the use of natural and synthetic nonsense suppressors. *J. Mol. Biol. 212*, 295−318.
(66) Markiewicz, P., Kleina, L. G., Cruz, C., Ehret, S., and Miller, J. H. (1994) Genetic studies of the lac repressor. XIV. Analysis of 4000 altered Escherichia coli lac repressors reveals essential and non-essential residues, as well as "spacers" which do not require a specific sequence. *J. Mol. Biol. 240*, 421−433.
(67) Nikaido, H. (2003) Molecular basis of bacterial outer membrane permeability revisited. *Microbiol. Molecul. Biol. Rev. 67*, 593−656.
(68) Basle, A., Rummel, G., Storici, P., Rosenbusch, J. P., and Schirmer, T. (2006) Crystal structure of osmoporin OmpC from E. coli at 2.0 A. *J. Mol. Biol. 362*, 933−942.
(69) Xu, Z., and Lee, S. Y. (1999) Display of polyhistidine peptides on the Escherichia coli cell surface by using outer membrane protein C as an anchoring motif. *Appl. Environ. Microbiol. 65*, 5142−5147.

DOI: 10.1021/acssynbio.6b00138
ACS Synth. Biol. XXXX, XXX, XXX−XXX

(70) Ashkenazy, H., Erez, E., Martz, E., Pupko, T., and Ben-Tal, N. (2010) ConSurf 2010: calculating evolutionary conservation in sequence and structure of proteins and nucleic acids. *Nucleic Acids Res. 38*, W529−533.
(71) Hoffmann, J. E., Plass, T., Nikic, I., Aramburu, I. V., Koehler, C., Gillandt, H., Lemke, E. A., and Schultz, C. (2015) Highly Stable trans-Cyclooctene Amino Acids for Live-Cell Labeling. *Chem. - Eur. J. 21*, 12266−12270.
(72) Versteegen, R. M., Rossin, R., ten Hoeve, W., Janssen, H. M., and Robillard, M. S. (2013) Click to release: instantaneous doxorubicin elimination upon tetrazine ligation. *Angew. Chem., Int. Ed. 52*, 14112−14116.
(73) Li, J., Jia, S., and Chen, P. R. (2014) Diels-Alder reaction-triggered bioorthogonal protein decaging in living cells. *Nat. Chem. Biol. 10*, 1003−1005.
(74) Pott, M., Schmidt, M. J., and Summerer, D. (2014) Evolved sequence contexts for highly efficient amber suppression with noncanonical amino acids. *ACS Chem. Biol. 9*, 2815−2822.
(75) Xu, H., Wang, Y., Lu, J., Zhang, B., Zhang, Z., Si, L., Wu, L., Yao, T., Xia, Q., Zhang, C., Xiao, S., Zhang, L., and Zhou, D. (2016) Re-exploration of the codon context effect on amber codon-guided incorporation of non-canonical amino acids in E. coli by the blue-white screening assay. *ChemBioChem 17*, 1250−1256.
(76) Johnson, D. B., Xu, J., Shen, Z., Takimoto, J. K., Schultz, M. D., Schmitz, R. J., Xiang, Z., Ecker, J. R., Briggs, S. P., and Wang, L. (2011) RF1 knockout allows ribosomal incorporation of unnatural amino acids at multiple sites. *Nat. Chem. Biol. 7*, 779−786.
(77) Wang, J., Kwiatkowski, M., and Forster, A. C. (2015) Kinetics of tRNA -mediated amber suppression in Escherichia coli translation reveals unexpected limiting steps and competing reactions. *Biotechnol. Bioeng. 113*, 1552−1559.
(78) O'Donoghue, P., Prat, L., Heinemann, I. U., Ling, J., Odoi, K., Liu, W. R., and Soll, D. (2012) Near-cognate suppression of amber, opal and quadruplet codons competes with aminoacyl-tRNAPyl for genetic code expansion. *FEBS Lett. 586*, 3931−3937.
(79) Plass, T., Milles, S., Koehler, C., Szymanski, J., Mueller, R., Wiessler, M., Schultz, C., and Lemke, E. A. (2012) Amino acids for Diels-Alder reactions in living cells. *Angew. Chem., Int. Ed. 51*, 4166−4170.
(80) Nikaido, H., and Vaara, M. (1985) Molecular basis of bacterial outer membrane permeability. *Microbiol. Rev. 49*, 1−32.
(81) Gilbert, W., and Muller-Hill, B. (1966) Isolation of the lac repressor. *Proc. Natl. Acad. Sci. U. S. A. 56*, 1891−1898.
(82) Schmitz, A., Schmeissner, U., and Miller, J. H. (1976) Mutations affecting the quaternary structure of the lac repressor. *J. Biol. Chem. 251*, 3359−3366.
(83) Brenowitz, M., Mandal, N., Pickar, A., Jamison, E., and Adhya, S. (1991) DNA-binding properties of a lac repressor mutant incapable of forming tetramers. *J. Biol. Chem. 266*, 1281−1288.
(84) Chakerian, A. E., Tesmer, V. M., Manly, S. P., Brackett, J. K., Lynch, M. J., Hoh, J. T., and Matthews, K. S. (1991) Evidence for leucine zipper motif in lactose repressor protein. *J. Biol. Chem. 266*, 1371−1374.
(85) Kania, J., and Brown, D. T. (1976) The functional repressor parts of a tetrameric lac repressor-beta-galactosidase chimaera are organized as dimers. *Proc. Natl. Acad. Sci. U. S. A. 73*, 3529−3533.
(86) Pedersen, W. T., and Curran, J. F. (1991) Effects of the nucleotide 3′ to an amber codon on ribosomal selection rates of suppressor tRNA and release factor-1. *J. Mol. Biol. 219*, 231−241.
(87) Cridge, A. G., Major, L. L., Mahagaonkar, A. A., Poole, E. S., Isaksson, L. A., and Tate, W. P. (2006) Comparison of characteristics and function of translation termination signals between and within prokaryotic and eukaryotic organisms. *Nucleic Acids Res. 34*, 1959−1973.
(88) Poole, E. S., Brown, C. M., and Tate, W. P. (1995) The identity of the base following the stop codon determines the efficiency of in vivo translational termination in Escherichia coli. *EMBO J. 14*, 151−158.
(89) Ueda, K., Yamamoto, Y., Ogawa, K., Abo, T., Inokuchi, H., and Aiba, H. (2002) Bacterial SsrA system plays a role in coping with unwanted translational readthrough caused by suppressor tRNAs. *Genes Cells 7*, 509−519.
(90) Korkmaz, G., Holm, M., Wiens, T., and Sanyal, S. (2014) Comprehensive analysis of stop codon usage in bacteria and its correlation with release factor abundance. *J. Biol. Chem. 289*, 30334−30342.
(91) Kozma, E., Nikic, I., Varga, B. R., Aramburu, I. V., Kang, J. H., Fackler, O. T., Lemke, E. A., and Kele, P. (2016) Hydrophilic trans-Cyclooctenylated Noncanonical Amino Acids for Fast Intracellular Protein Labeling. *ChemBioChem 17*, 1518−1524.
(92) Stagge, F., Mitronova, G. Y., Belov, V. N., Wurm, C. A., and Jakobs, S. (2013) SNAP-, CLIP- and Halo-tag labelling of budding yeast cells. *PLoS One 8*, e78745.
(93) Crawford, R., Torella, J. P., Aigrain, L., Plochowietz, A., Gryte, K., Uphoff, S., and Kapanidis, A. N. (2013) Long-lived intracellular single-molecule fluorescence using electroporated molecules. *Biophys. J. 105*, 2439−2450.
(94) Pages, J. M., James, C. E., and Winterhalter, M. (2008) The porin and the permeating antibiotic: a selective diffusion barrier in Gram-negative bacteria. *Nat. Rev. Microbiol. 6*, 893−903.
(95) Evans, L. J., Cooper, A., and Lakey, J. H. (1996) Direct measurement of the association of a protein with a family of membrane receptors. *J. Mol. Biol. 255*, 559−563.
(96) Link, A. J., and Tirrell, D. A. (2003) Cell surface labeling of Escherichia coli via copper(I)-catalyzed [3 + 2] cycloaddition. *J. Am. Chem. Soc. 125*, 11164−11165.
(97) Morona, R., Tommassen, J., and Henning, U. (1985) Demonstration of a bacteriophage receptor site on the Escherichia coli K12 outer-membrane protein OmpC by the use of a protease. *Eur. J. Biochem. 150*, 161−169.
(98) Misra, R., Peterson, A., Ferenci, T., and Silhavy, T. J. (1991) A genetic approach for analyzing the pathway of LamB assembly into the outer membrane of Escherichia coli. *J. Biol. Chem. 266*, 13592−13597.
(99) Jansen, C., Wiese, A., Reubsaet, L., Dekker, N., de Cock, H., Seydel, U., and Tommassen, J. (2000) Biochemical and biophysical characterization of in vitro folded outer membrane porin PorA of Neisseria meningitidis. *Biochim. Biophys. Acta, Biomembr. 1464*, 284−298.
(100) McKinney, S. A., Murphy, C. S., Hazelwood, K. L., Davidson, M. W., and Looger, L. L. (2009) A bright and photostable photoconvertible fluorescent protein. *Nat. Methods 6*, 131−133.
(101) Mizuno, T., Chou, M. Y., and Inouye, M. (1983) DNA sequence of the promoter region of the ompC gene and the amino acid sequence of the signal peptide of pro-OmpC protein of Escherichia coli. *FEBS Lett. 151*, 159−164.
(102) Gold, V. A., Duong, F., and Collinson, I. (2007) Structure and function of the bacterial Sec translocon. *Mol. Membr. Biol. 24*, 387−394.
(103) Feilmeier, B. J., Iseminger, G., Schroeder, D., Webber, H., and Phillips, G. J. (2000) Green fluorescent protein functions as a reporter for protein localization in Escherichia coli. *J. Bacteriol. 182*, 4068−4076.
(104) Dammeyer, T., and Tinnefeld, P. (2012) Engineered fluorescent proteins illuminate the bacterial periplasm. *Comput. Struct. Biotechnol. J. 3*, e201210013.
(105) Schnaitman, C. A., and McDonald, G. A. (1984) Regulation of outer membrane protein synthesis in Escherichia coli K-12: deletion of ompC affects expression of the OmpF protein. *J. Bacteriol. 159*, 555−563.
(106) Voulhoux, R., Bos, M. P., Geurtsen, J., Mols, M., and Tommassen, J. (2003) Role of a highly conserved bacterial protein in outer membrane protein assembly. *Science 299*, 262−265.
(107) Wu, T., Malinverni, J., Ruiz, N., Kim, S., Silhavy, T. J., and Kahne, D. (2005) Identification of a multicomponent complex required for outer membrane biogenesis in Escherichia coli. *Cell 121*, 235−245.

DOI: 10.1021/acssynbio.6b00138
ACS Synth. Biol. XXXX, XXX, XXX−XXX

(108) Sheridan, D. L., Berlot, C. H., Robert, A., Inglis, F. M., Jakobsdottir, K. B., Howe, J. R., and Hughes, T. E. (2002) A new way to rapidly create functional, fluorescent fusion proteins: random insertion of GFP with an in vitro transposition reaction. *BMC Neurosci. 3*, 7.
(109) Kusumi, A., Tsunoyama, T. A., Hirosawa, K. M., Kasai, R. S., and Fujiwara, T. K. (2014) Tracking single molecules at work in living cells. *Nat. Chem. Biol. 10*, 524−532.
(110) Suzuki, K., Ritchie, K., Kajikawa, E., Fujiwara, T., and Kusumi, A. (2005) Rapid hop diffusion of a G-protein-coupled receptor in the plasma membrane as revealed by single-molecule techniques. *Biophys. J. 88*, 3659−3680.
(111) Wieser, S., and Schutz, G. J. (2008) Tracking single molecules in the live cell plasma membrane-Do's and Don't's. *Methods 46*, 131−140.
(112) Kusumi, A. (1994) Confined Lateral Diffusion of Membrane-Receptors as Studied by Single-Particle Tracking and Laser Tweezers. *Biophys. J. 66*, A18.
(113) Robson, A., Burrage, K., and Leake, M. C. (2013) Inferring diffusion in single live cells at the single-molecule level. *Philos. Trans. R. Soc., B 368*, 20120029.
(114) Ritchie, K., Shan, X. Y., Kondo, J., Iwasawa, K., Fujiwara, T., and Kusumi, A. (2005) Detection of non-Brownian diffusion in the cell membrane in single molecule tracking. *Biophys. J. 88*, 2266−2277.
(115) Sanamrad, A., Persson, F., Lundius, E. G., Fange, D., Gynna, A. H., and Elf, J. (2014) Single-particle tracking reveals that free ribosomal subunits are not excluded from the Escherichia coli nucleoid. *Proc. Natl. Acad. Sci. U. S. A. 111*, 11413−11418.
(116) Saxton, M. J., and Jacobson, K. (1997) Single-particle tracking: Applications to membrane dynamics. *Annu. Rev. Biophys. Biomol. Struct. 26*, 373−399.
(117) Kumar, M., Mommer, M. S., and Sourjik, V. (2010) Mobility of cytoplasmic, membrane, and DNA-binding proteins in Escherichia coli. *Biophys. J. 98*, 552−559.
(118) Lenn, T., Leake, M. C., and Mullineaux, C. W. (2008) Clustering and dynamics of cytochrome bd-I complexes in the Escherichia coli plasma membrane in vivo. *Mol. Microbiol. 70*, 1397−1407.
(119) Leake, M. C., Greene, N. P., Godun, R. M., Granjon, T., Buchanan, G., Chen, S., Berry, R. M., Palmer, T., and Berks, B. C. (2008) Variable stoichiometry of the TatA component of the twin-arginine protein transport system observed by in vivo single-molecule imaging. *Proc. Natl. Acad. Sci. U. S. A. 105*, 15376−15381.
(120) Lommerse, P. H., Blab, G. A., Cognet, L., Harms, G. S., Snaar-Jagalska, B. E., Spaink, H. P., and Schmidt, T. (2004) Single-molecule imaging of the H-ras membrane-anchor reveals domains in the cytoplasmic leaflet of the cell membrane. *Biophys. J. 86*, 609−616.
(121) Sako, Y., and Kusumi, A. (1994) Compartmentalized structure of the plasma membrane for receptor movements as revealed by a nanometer-level motion analysis. *J. Cell Biol. 125*, 1251−1264.
(122) Oddershede, L., Dreyer, J. K., Grego, S., Brown, S., and Berg-Sorensen, K. (2002) The motion of a single molecule, the lambda-receptor, in the bacterial outer membrane. *Biophys. J. 83*, 3152−3161.
(123) Gibbs, K. A., Isaac, D. D., Xu, J., Hendrix, R. W., Silhavy, T. J., and Theriot, J. A. (2004) Complex spatial distribution and dynamics of an abundant Escherichia coli outer membrane protein, LamB. *Mol. Microbiol. 53*, 1771−1783.
(124) Yamada, H., and Mizushima, S. (1981) The Assembly of a Major Outer-Membrane Protein (Ompf) in the Cell-Surface of Escherichia-Coli. *Agric. Biol. Chem. 45*, 2083−2090.
(125) Nogami, T., and Mizushima, S. (1983) Outer-Membrane Porins Are Important in Maintenance of the Surface-Structure of Escherichia-Coli-Cells. *J. Bacteriol. 156*, 402−408.
(126) Lenn, T., Leake, M. C., and Mullineaux, C. W. (2008) Are Escherichia coli OXPHOS complexes concentrated in specialized zones within the plasma membrane? *Biochem. Soc. Trans. 36*, 1032−1036.
(127) Nenninger, A., Mastroianni, G., Robson, A., Lenn, T., Xue, Q., Leake, M. C., and Mullineaux, C. W. (2014) Independent mobility of proteins and lipids in the plasma membrane of Escherichia coli. *Mol. Microbiol. 92*, 1142−1153.
(128) Hong, S. H., Ntai, I., Haimovich, A. D., Kelleher, N. L., Isaacs, F. J., and Jewett, M. C. (2014) Cell-free protein synthesis from a release factor 1 deficient Escherichia coli activates efficient and multiple site-specific nonstandard amino acid incorporation. *ACS Synth. Biol. 3*, 398−409.
(129) Heinemann, I. U., Rovner, A. J., Aerni, H. R., Rogulina, S., Cheng, L., Olds, W., Fischer, J. T., Soll, D., Isaacs, F. J., and Rinehart, J. (2012) Enhanced phosphoserine insertion during Escherichia coli protein synthesis via partial UAG codon reassignment and release factor 1 deletion. *FEBS Lett. 586*, 3716−3722.
(130) Mukai, T., Hoshi, H., Ohtake, K., Takahashi, M., Yamaguchi, A., Hayashi, A., Yokoyama, S., and Sakamoto, K. (2015) Highly reproductive Escherichia coli cells with no specific assignment to the UAG codon. *Sci. Rep. 5*, 9699.
(131) Fan, C., Xiong, H., Reynolds, N. M., and Soll, D. (2015) Rationally evolving tRNAPyl for efficient incorporation of non-canonical amino acids. *Nucleic Acids Res. 43*, e156.
(132) Schmied, W. H., Elsasser, S. J., Uttamapinant, C., and Chin, J. W. (2014) Efficient multisite unnatural amino acid incorporation in mammalian cells via optimized pyrrolysyl tRNA synthetase/tRNA expression and engineered eRF1. *J. Am. Chem. Soc. 136*, 15577−15583.
(133) Bell, C. E., and Lewis, M. (2000) A closer view of the conformation of the Lac repressor bound to operator. *Nat. Struct. Biol. 7*, 209−214.
(134) Ullman, G., Wallden, M., Marklund, E. G., Mahmutovic, A., Razinkov, I., and Elf, J. (2013) High-throughput gene expression analysis at the level of single proteins using a microfluidic turbidostat and automated cell tracking. *Philos. Trans. R. Soc., B 368*, 20120025.
(135) Sadanandan, S. K., Baltekin, O., Magnusson, K. E. G., Boucharin, A., Ranefall, P., Jalden, J., Elf, J., and Wahlby, C. (2016) Segmentation and Track-Analysis in Time-Lapse Imaging of Bacteria. *Ieee J-Stsp 10*, 174−184.
(136) Olivo-Marin, J. C. (2002) Extraction of spots in biological images using multiscale products. *Pattern Recognit. 35*, 1989−1996.
(137) Sadler, B. M., and Swami, A. (1999) Analysis of multiscale products for step detection and estimation. *IEEE Trans. Inf. Theory 45*, 1043−1051.
(138) Martin, D. S., Forstner, M. B., and Kas, J. A. (2002) Apparent subdiffusion inherent to single particle tracking. *Biophys. J. 83*, 2109−2117.

DOI: 10.1021/acssynbio.6b00138
ACS Synth. Biol. XXXX, XXX, XXX−XXX